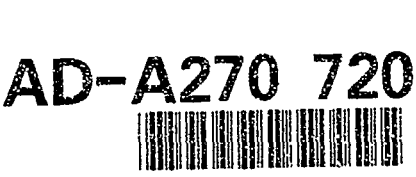

ARMY RESEARCH LABORATORY

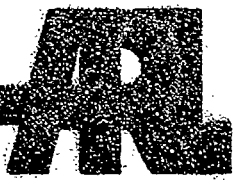

Detailed Structure Study of an $H_2/N_2O/Ar$ Flame Employing Molecular Beam Mass Spectrometry, Laser Spectroscopy, and Modeling

Rosario C. Sausa
David C. Dayton
William R. Anderson
Cynthia M. Faust
Stephen L. Howard

ARL-TR-232 October 1993

NOTICES

Destroy this report when it is no longer needed. DO NOT return it to the originator.

Additional copies of this report may be obtained from the National Technical Information Service, U.S. Department of Commerce, 5285 Port Royal Road, Springfield, VA 22161.

The findings of this report are not to be construed as an official Department of the Army position, unless so designated by other authorized documents.

The use of trade names or manufacturers' names in this report does not constitute indorsement of any commercial product.

REPORT DOCUMENTATION PAGE

Form Approved
OMB No. 0704-0188

1. AGENCY USE ONLY (Leave blank)	2. REPORT DATE	3. REPORT TYPE AND DATES COVERED
	October 1993	Final, Jun 92 - Jan 93

4. TITLE AND SUBTITLE

Detailed Structure Study of an $H_2/N_2O/Ar$ Flame Employing Molecular Beam Mass Spectrometry, Laser Spectroscopy, and Modeling

5. FUNDING NUMBERS

PR: 1L161102AH43

6. AUTHOR(S)

Rosario C. Sausa, David C. Dayton, William R. Anderson, Cynthia M. Faust, and Stephen L. Howard

7. PERFORMING ORGANIZATION NAME(S) AND ADDRESS(ES)

U.S. Army Research Laboratory
ATTN: AMSRL-WT-PC
Aberdeen Proving Ground, MD 21005-5066

8. PERFORMING ORGANIZATION REPORT NUMBER

9. SPONSORING/MONITORING AGENCY NAME(S) AND ADDRESS(ES)

U.S. Army Research Laboratory
ATTN: AMSRL-OP-CI-B (Tech Lib)
Aberdeen Proving Ground, MD 21005-5066

10. SPONSORING/MONITORING AGENCY REPORT NUMBER

ARL-TR-232

11. SUPPLEMENTARY NOTES

12a. DISTRIBUTION/AVAILABILITY STATEMENT

Approved for public release; distribution is unlimited.

12b. DISTRIBUTION CODE

13. ABSTRACT *(Maximum 200 words)*

A combined experimental and detailed chemical modeling study has been performed on a 20-torr, stoichiometric $H_2/N_2O/Ar$ burner stabilized flame. This study provides a check of part of the mechanism to be used in models for the combustion of solid nitramine propellants. Species concentration profiles were measured using molecular beam sampling with mass spectrometric detection and laser-induced fluorescence, while temperature profiles were measured with coated Pt/Pt-Rh(10%) thermocouples. The burned gases of the flame contain about 2 mole % of NO and H_2, a concentration of approximately 10 times more than that of their equilibrium. This formation prevents full energy release of the system within or near the flame zone. Experimental flame profiles of the major species, H_2, N_2O, N_2, and H_2O, as well as the minor species, NO, O_2, OH, H, O, and NH, are presented and compared to calculated profiles generated by PREMIX, a one-dimensional premixed laminar flame code. The chemical mechanism used in the flame code was derived from a critical literature review and consists of 38 reactions and 14 species. Rate and sensitivity analyses performed reveal the intricacies of the mechanism as well as reactions important in the modeling of the experimental results. Several key reactions, including $N_2O + OH = HO_2 + N_2$ and $N_2O + H = NO + NH$, whose rate coefficients have been controversial, are discussed in detail. In addition, the importance of various collision partners in the key initiation step, $N_2O + M = N_2 + O + M$, is presented and discussed.

14. SUBJECT TERMS

mass spectrometry, laser spectroscopy, molecular beam sampling, hydrogen/nitrous, oxides, flames, PREMIX, rate analysis, sensitivity analysis, thermocouples, chemical mechanism

15. NUMBER OF PAGES

50

16. PRICE CODE

17. SECURITY CLASSIFICATION OF REPORT	18. SECURITY CLASSIFICATION OF THIS PAGE	19. SECURITY CLASSIFICATION OF ABSTRACT	20. LIMITATION OF ABSTRACT
UNCLASSIFIED	UNCLASSIFIED	UNCLASSIFIED	SAR

INTENTIONALLY LEFT BLANK.

ACKNOWLEDGMENTS

The authors thank Dr. Gregory Smith (SRI) for sending his mechanism for H_2/N_2O combustion, Dr. Anthony Kotlar (ARL) for helping us run his fitting program which was used to smooth the temperature profile, and one of the referees for his (her) constructive suggestions and comments. They also thank Drs. Terence P. Coffee (ARL), James A. Miller (Sandia), and John D. Powell (ARL) for many valuable discussions, Mr. Steve W. Haga for writing most of the postprocessor code, and Dr. Andrzej W. Miziolek (ARL) for review of the manuscript. Support from the NRC/ARL Postdoctoral Research Program (SLH, DCD, and CMF), ARL Combustion Mission Program (RCS and WRA), Productivity Capital Investment Program (RCS and WRA), and partial support from the Office of Naval Research (RCS), Grant Number MIPR-N0001490-MP-24054, is acknowledged.

INTENTIONALLY LEFT BLANK.

TABLE OF CONTENTS

INTENTIONALLY LEFT BLANK.

LIST OF FIGURES

INTENTIONALLY LEFT BLANK.

1. INTRODUCTION

The combustion of nitrogen-containing species has been of fundamental interest for over three decades (Gaydon 1974; Gaydon and Wolfhard 1949; Wolfhard and Parker 1955). Much of the interest is directed towards understanding and predicting pollutant formation. Our interest in nitrogen combustion stems from a desire to model propellant combustion, primarily solid nitramines or nitrocellulose-based types. A fundamental understanding of the detailed chemistry is a prerequisite for the successful modeling of propellant combustion which will lead to optimal propellant formulation and propulsion performance. Of foremost importance are molecules such as N_2O and NO_2, since they are intermediate oxidizers formed during propellant combustion (Fifer 1984; Schroeder 1985). Thus, one of the simplest flame chemical systems of interest to both propellant chemistry and pollutant formation is the H_2/N_2O system.

Several flame studies have been performed on the H_2/N_2O system. Fine and Evans (1963) measured NO concentrations and temperature in the burned gases of flames using a number of fuels, including H_2 with N_2O. The results were used to infer qualitative information about reactions responsible for NO formation under a wide variety of conditions. In a number of other early studies (Dixon-Lewis, Sutton, and Williams 1964, 1965a, 1965b; Duval and Van Tiggelen 1967), flame speeds and a few species and temperature profiles were also measured. More recently, Cattolica, Smooke, and Dean (1982) performed a combined modeling and experimental study for a flat, burner stabilized, stoichiometric, atmospheric pressure H_2/N_2O flame. Laser-induced fluorescence (LIF) and absorption spectroscopy were used to obtain concentration profiles of OH, NH, and NO, as well as a temperature profile. However, the measurements could only be performed in the upper portions of the flame zone. Subsequent studies on a similar burner by Vanderhoff et al. (1986) yielded profiles for NO, O_2, N_2, and temperature using Raman spectroscopy and relative OH profiles using LIF for several H_2/N_2O flames ranging from lean to stoichiometric mixture ratios at atmospheric pressure.

Generally, species profiles obtained in the atmospheric pressure studies were poorly resolved. However, an increase in spatial resolution can be obtained at reduced pressures since the reaction zone expands. The first low-pressure work which combined an experimental and theoretical study was performed by Balakhnin, Vandooren, and Van Tiggelen (1977) on the structure of a lean H_2/N_2O flame (31.4% H_2) at 40 torr. Molecular beam sampling with mass spectrometric detection (MB/MS) was employed to profile all of the stable and most of the reactive species. Using an assumed mechanism, consisting of approximately a dozen reactions, several bimolecular rate constants were deduced and the

importance of the N_2O+M decomposition reaction was discussed. A concentration profile of the NH radical was not reported and, as a result, the NH chemistry was excluded from the mechanism. Recently, several hydrogen flames (Kohse-Höinghaus et al. 1988; Rensberger et al. 1988; Jefferies et al. 1988) supported by N_2O or O_2 at low pressure have been studied in which the NH radical profiles have been obtained. For one of the H_2/N_2O flames, the temperature profile as well as the OH and NH radical profiles were obtained by LIF and modeled (Jefferies et al. 1988). A very brief discussion of the chemistry is given, but the major emphasis of that work was to determine the influence of temperature and majority species mixture on quenching of the LIF signals for these radicals.

In a modeling study, Coffee (1986) developed a model for premixed, one-dimensional flames and calculated flame speeds and species profiles for a variety of H_2/N_2O flames. The results were compared to a range of previously published experimental data and revealed that his model reproduces the data overall, but inaccuracies still exist. In particular, most of the predicted flame speeds were slightly slower than experiment. Sensitivity and rate analyses were used to indicate that additional experimental data, particularly on OH and NO, were needed to improve his model.

In addition to the flame studies, there have been several shock tube (Henrici and Bauer 1969; Dean 1976; Dean, Steiner, and Wang 1978; Pamidimukkala and Skinner 1982; Hidaka, Takuma, and Suga 1985a, 1985b) and bulb (Baldwin, Gethin, and Walker 1973; Baldwin, Gethin, and Plaistowe 1975) studies on the H_2/N_2O chemical system. In the shock tube studies, conditions were tailored primarily to highlight one or a few of the elementary reaction steps and to measure the corresponding rate coefficients. The bulb experiments examined the chemical mechanism for this system at low temperatures.

Presented in this report are temperature and species profile measurements for a 20-torr stoichiometric H_2/N_2O/Ar burner stabilized flame. MB/MS and LIF are used to measure a variety of stable and reactive radical species. The low pressure attained enables high spatial resolution profiles to be obtained through the entire flame zone. A wider variety of species profiles has been obtained than has previously appeared for any study of this chemical system due largely to the use of the MB/MS system. The experimental data is compared to calculated profiles generated using the Sandia National Laboratories flame code, PREMIX (Kee et al. 1991). The mechanism used to generate the model profiles is the result of a detailed examination of the literature concerning gas-phase nitrogen combustion. Rate and sensitivity analyses performed reveal the intricacies of the mechanism. The main features of the mechanism are presented and reactions of particular interest highlighted.

2. EXPERIMENTAL

A schematic of the experimental apparatus is shown in Figure 1. The H_2/N_2O/Ar low-pressure flame was supported on a McKenna flat burner having a 6-cm stainless-steel fritted plug. The plug is encircled by another sintered metal frit through which argon was flowed, thus forming a protective shroud that minimized mixing of any recirculating burnt gases in the low-pressure chamber. The center plug was water cooled to maintain a constant temperature as measured by imbedded Alumel-Chromel thermocouples. The burner was mounted at the center of a cylindrical stainless-steel vacuum chamber (D=25 cm, H=40 cm) on a high vacuum feedthrough flange which was coupled to an off-axis rotary feedthrough flange. This configuration allowed the burner to be scanned vertically with an accuracy and reproducibility of less than 50 μm and horizontally with a rotational precision of better than 1°.

The reactant gases (H_2 and N_2O) and inert gas (Ar) were of commercial high-purity grade and were metered by MKS mass flow controllers (cross-checked with a GCA Precision Scientific wet test meter). The gas flow rates employed were 1.6 and 1.4 L/min (STP) for the reactant gases and diluent, respectively, corresponding to a mass flow rate of 3.41×10^{-3} g/cm^2/s. Pressures ranging from 5 to 25 torr were maintained with a D-40 Leybold-Heraeus vacuum pump and measured with a MKS 270 baratron (390HA pressure head) interfaced to a MKS 252 pressure controller and exhaust throttle valve. For this study, the flame was stabilized on the burner at a pressure of 20 torr. Under these conditions, the flame was characterized by a dark preheat zone and a pale yellow luminous zone. The dark or nonluminous zone is approximately 5 mm high and occurs at the surface of the burner where the gas temperature is relatively low. The luminous zone is approximately 5–8 mm high. The thickness of the zones could be altered by changing the relative proportions of the reactants and argon diluent, as well as the pressure.

Temperature profiles of the H_2/N_2O flame were obtained with thermocouples. Platinum and platinum with 10% rhodium wires of 125 μm diameters were spot-welded to produce a thermocouple junction and mounted at 180° on a "V" shaped holder equipped with a spring to eliminate any sag when placed in the flame. The thermocouples were coated with a beryllium oxide (15%)/yttrium oxide mixture following a procedure reported by J. H. Kent (1970) to avoid surface catalytic effects. The temperature was measured as the burner traversed the distance from the thermocouple in the forward and reverse directions. Scanning the burner in both directions yielded temperatures which varied by less than ±5 K. The average

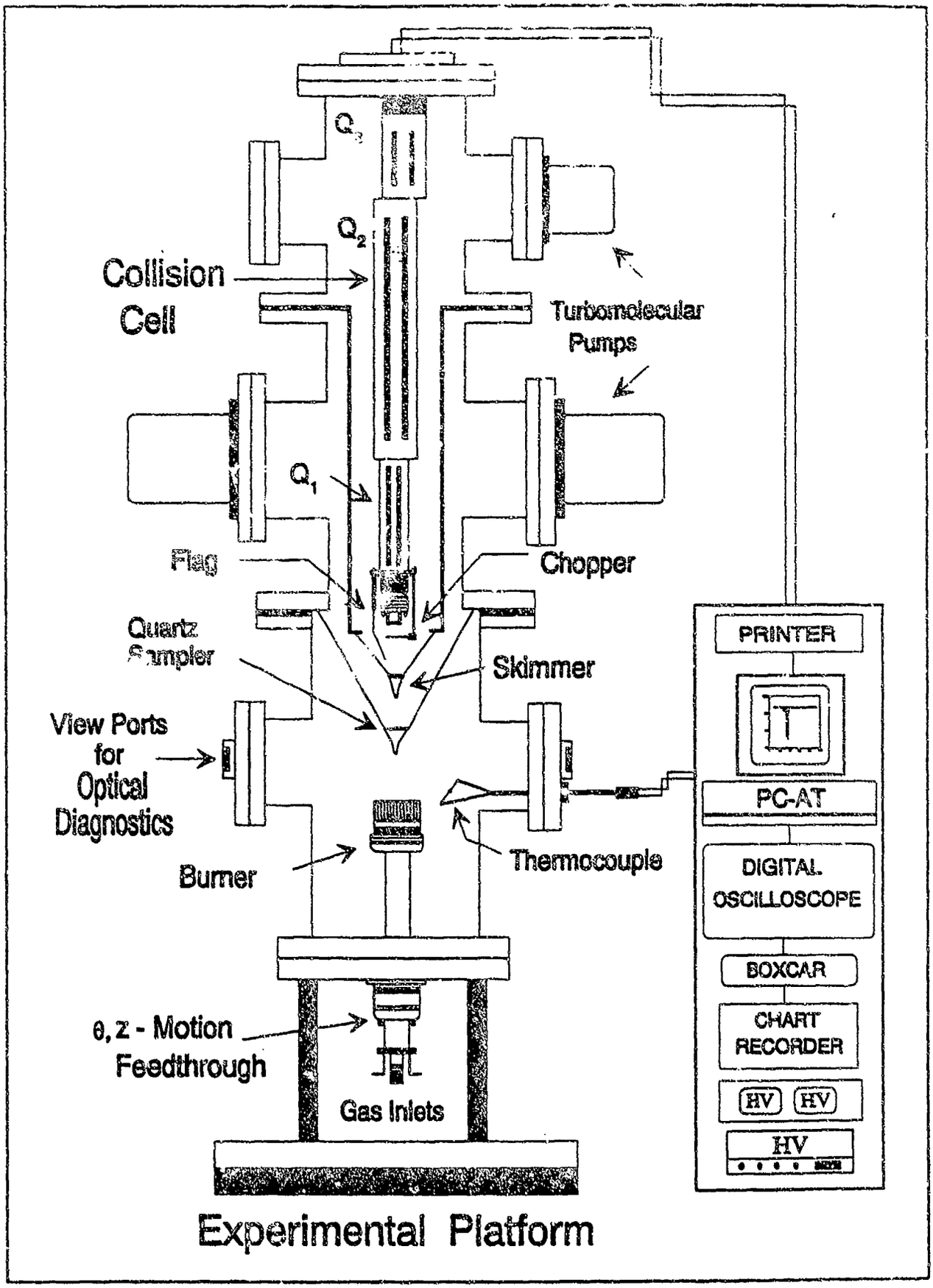

Figure 1. Schematic of the experimental apparatus.

temperature was then corrected for thermocouple radiation losses using the following equation (Fristrom and Westenberg 1965),

$$\Delta T = T_{cal} - T_{obs} = \varepsilon\sigma d(T^4 - T_o^4)/2k \quad , \qquad (1)$$

where ε is the emissivity of the coated thermocouple, σ is the Stefan-Boltzmann constant, d is the diameter of the coated junction, k is the thermal conductivity of the flame gases, and T_o is 300 K. The above equation is for a spherical thermocouple junction with a small enough diameter that its Reynolds number is much less than 1. A measured diameter of 190 μm for the coated thermocouple junction and an emissivity value of 0.6 reported by Peterson (1981) were employed in the correction. The reported emissivity value has an uncertainty of ±12.5% and is in good agreement with the value of 0.64 reported by Seery and Zabielski (1977). Considering the uncertainty in the emissivity value, the maximum error in the corrected temperature due to this factor is approximately 1%. The overall uncertainty of the temperature measurements is ± 50 K in the region of peak temperature where the correction term is largest (approximately 200 K) and within 20 K in the preheat region. The sodium line reversal (SLR) technique, described in a previous publication (Bernstein et al. 1993), was used to crosscheck the thermocouple temperature measurements. Flame temperatures were measured in a 20-torr $C_2H_4/O_2/Ar$ flame with the same thermocouple and using the SRL technique. After correcting for the thermocouple's radiation losses, the temperature measurements were within the reported experimental uncertainty.

MB/MS was employed to monitor the stable and radical species. The mass spectrometer system consists of an Extrel C50 TQMS inline triple quadruple mass filter with a concentric-axis ionizer as shown schematically in Figure 1. For this study, the triple quadruple was operated as a single quadruple with mass filtering by either the first or third quadruple. Flame gases were sampled through a conical quartz skimmer with a 200-μm-diameter orifice. The gases expanded supersonically into the first differential vacuum chamber with a background pressure of 5×10^{-5} torr. The expanding gases were then collimated through a second skimmer (Beam Dynamics Model 2, 2-mm orifice diameter) and passed into the ionization region of the first quadruple, maintained at a pressure of 2×10^{-6} torr. The beam was then modulated at 200 Hz with a tuning fork chopper and ionized prior to entering the first quadruple (ionization energy was 17.0 ± 0.1 eV and electron current maintained at 0.1 ± 0.01 mA except where noted). A beamstop was included to determine if the modulated beam was a molecular beam (modulation would cease with beamstop activated) or an effusive beam (no change in modulation noted with beamstop activated). The ion current was measured with a continuous-dynode electron multiplier and processed with

a lock-in amplifier (Stanford Research System Model SR530). Phase-sensitive detection allowed discrimination of background gases and signal averaging to increase sensitivity.

The concentration of stable species was determined by direct calibration at ambient temperature by a procedure reported by Peeters and Mahnen (1973). The relationship between the signal intensity of a given species and the partial pressure can be expressed as

$$I_i = S_i P_i \quad , \tag{2}$$

where S_i is the overall sensitivity factor of the apparatus which takes into account the ionization cross section. It is assumed that S_i varies for all species as a function of pressure, temperature, and mean molecular weight of the sampled gas in the same manner. Therefore, the ratio of sensitivities of any two species, S_i/S_j, remains constant at every point in the flame and is equal to that obtained at ambient temperature. This assumption was verified by introducing a known concentration of He in the $H_2/N_2O/Ar$ low-pressure flame and measuring the (S_{He}/S_{Ar}) ratio along the flame zone and at ambient temperature. The uncertainty in the stable species concentration is estimated as ± 10%.

The degree of perturbation introduced by the sampler was checked by monitoring the OH radical using laser-induced fluorescence. The radical was monitored by employing the $R_1(6.5)$ and $R_1(7.5)$ rotational lines of its $A^2\Sigma^+ - X^2\Pi_i$ (1,0) electronic transition near 281 nm. These rotational transitions are least sensitive to temperature, particularly in regions of large temperature gradient, as evidenced by Equation 3 (Eckbreth 1988),

$$J^2 + J - (k/hcB_v)T_{av} = 0 \quad , \tag{3}$$

where J is the rotational level; k, h, c, and B_v are the usual spectroscopic constants; and T_{av} is the average flame temperature. The (1,0) band was chosen over the stronger (0,0) band near 306 nm in order to minimize self absorption. Overall, the profiles obtained by the two techniques are in good agreement. Both techniques yielded reliable species profile data in the flame front and burned gas zone. However, in the preheat zone, near the burner surface, the quartz probe perturbs the flame slightly. Similar findings were reported in a previous study (Howard et al. 1992).

The probe beam was provided by an XeCl excimer-pumped dye laser (Lumonics HyperEX 400/HyperDYE 300) which was frequency doubled (HyperTRAK 1000) to obtain the required

UV wavelengths. The linewidth for UV radiation is approximately 0.16 cm^{-1} (fwhm). The probe beam was collimated with irises to a diameter of approximately 2.0 mm and focused over the center of the burner with a 500-mm focal length lens. The induced fluorescence, corresponding to the (1,1) transition, was collected 90° to the excitation laser beam and focused with a 300-mm focal length lens onto the entrance slit of a Hamamatsu R-955 photomultiplier equipped with a 15-nm fwhm interference filter centered at 311 nm (Corion). The resulting signal was then directed into a boxcar integrator (Stanford Research System 252) set for a 9-ns gate width in order to minimize the effects of collisional quenching and/or energy transfer of the rotationally excited states. The fluorescence signal was monitored on a 125-MHz digital oscilloscope (Lecroy 9400). A PC-AT computer was employed for data acquisition and analysis.

3. CODE AND COMPUTATIONAL DETAILS

The computations were performed with the code PREMIX (Ver. 1.4), developed at Sandia National Laboratories (Kee et al. 1991). This code uses CHEMKIN-II (Ver. 1.8), a library of user-friendly, chemistry-related subroutines and a chemical mechanism interpreter code designed to calculate problems involving elementary gas phase kinetics (Kee, Rupley, and Miller 1989). The equations for a one-dimensional, premixed, laminar, steady-state flame, which includes complex chemistry as well as gas-phase transport and thermodynamic properties, are solved to predict species concentration and temperature profiles as a function of distance above the burner surface. This code can be used to perform three different types of flame calculations: 1) free flame, 2) burner stabilized with normal boundary conditions, and 3) burner stabilized with infinite H-atom recombination rate to H_2 at the burner surface. The first two cases are readily available in the code while the third case is achieved by modifying the code's boundary equations (Warnatz 1978) for hydrogen boundary conditions (HBC) and has been implemented in the calculations presented in this report. For the present conditions, the solutions determined using either HBC or normal boundary conditions are identical except for the H atom profile close to the burner surface (<5 mm). The result for normal boundary conditions is, of course, that the H atom concentration is not zero at the burner surface. The calculations also include thermal diffusion for light species (H and H_2). A solution is regarded as acceptable when the following conditions are satisfied: 1) the flame front is far enough from the hot boundary that the boundary conditions do not affect the solution, 2) the error tolerances are sufficiently small, and 3) increasing the number of grid points will not alter the solution.

PREMIX extracts important gas-phase thermodynamic and transport properties for the species being considered from two databases provided by Sandia National Laboratories (Kee, Rupley, and Miller 1987; Kee et al. 1988). The reactions employed in the mechanism are written in the direction in which their rate expressions are more accurately known. We define this direction as the forward direction. At the user's discretion, CHEMKIN computes the rate constants of the reverse reactions by using thermodynamic properties and forward rate coefficients. As a result, thermodynamic databases can be important (Martin and Brown 1989). In the present work, several important NH reactions have been reversed. The thermodynamic properties for NH are well-known with the exception of the heat of formation, which has been a controversial subject. The value used in the database (Kee, Rupley, and Miller 1987), however, is very close to the recommended value found in a recent critical review (Anderson 1989). Version 1.4 of PREMIX incorporates the calculations of species transport properties using the transport property formulation (method VI) of Coffee and Heimerl (1981, 1983) to obtain species transport effects.

Recent work by Smith (1992) has demonstrated that expansion of the flame area above the burner can have a very important effect on the species profiles, especially the thickness of the flame zone. This is due to the residence time of the reacting gases (time it takes the gases to travel a given distance) which can be strongly affected by expansion. For present conditions, visual inspection of the flame indicated that the expansion ratio is no larger than 1.2 per cm. Test calculations incorporating this value as an upper limit in the flame code showed that the computed profiles are altered very little by this effect.

A post processor was written for the PREMIX code to analyze heat release as well as sensitivities and rates of reactions at discrete distances above the burner surface. The postprocessor calculates the net contribution of each reaction to the formation or removal rates of given species and sorts the reactions in decreasing order of importance. The PREMIX code calculates raw sensitivity coefficients for each reaction and species, which are normalized by the post processor according to the equation,

$$S_{ik} = A_i / X_{k,m} \, (\partial X_k / \partial A_i) \quad , \tag{4}$$

where S_{ik} is the normalized sensitivity coefficient, A_i is the Arrhenius A coefficient of reaction i, and $X_{k,m}$ is the maximum mole fraction of species k. These normalized sensitivity coefficients are sorted to determine which reactions have the greatest effect on a given species concentration.

The PREMIX flame code allows one to choose between using the measured temperature profile as a fixed input to the problem, thus generating the species profiles for comparison with experiment, or to solve the energy equation, thus obtaining a predicted temperature profile as part of the solution. The energy equation in PREMIX only accounts for conductive heat losses from the flame to the burner surface. Both approaches were tried. Although the fixed input approach was used to model the experimental species concentration profiles, two important points were found by examining the results obtained using the energy equation. First, a temperature of approximately 2,650 K is predicted for the burned gas just past the flame zone, approximately 200 K smaller than that predicted at a very long distance from the burner. That is, the postflame temperature is predicted to overshoot its value at equilibrium. A temperature overshoot of similar magnitude has been observed by Smith (1993) for a low-pressure H_2/N_2O flame. For our flame system, an overshoot is also predicted for the corresponding free flame calculation where the correct adiabatic flame temperature is attained at large distances. These unusual temperature overshoots are due to the predicted concentrations of H, O, and OH radicals in the flame zone. The typical radical overshoot is not predicted for these flames. Instead, the radical concentration is lower than the equilibrium value and rises slowly in the postflame region. The second point in solving the energy equation is that it results in a predicted final flame temperature that is approximately 500–600 K larger than that measured experimentally. Not surprisingly, the predicted flame zone width is much smaller. A 400–500 K difference is also observed by Smith (1993) in an independent study on the H_2/N_2O flame. Large differences are predicted for several other fuel/oxidizers as well. These results suggest that nonnegligible gas phase heat losses (for example, radiative) to the surroundings are not properly accounted for in the energy equation. Since the predicted temperature is so different from experiment, this approach cannot reasonably be used to model the results. It is clear that further study of the heat loss mechanism(s) is needed. For our system, it should be noted, however, that the magnitudes and relative ordering of sensitivities of the species profiles to reaction rate coefficients were found to be similar for both methods. This means that, perhaps surprisingly, the computed species profiles are nearly equally sensitive to the kinetics parameters for either approach.

4. RESULTS AND DISCUSSION

4.1 Chemical Mechanism. The gross chemical structure of H_2/N_2O flames can be characterized by a number of important reactions which have been discussed in previous studies (Cattolica, Smooke, and

Dean 1982; Balakhnin, Vandooren, and Van Tiggelen 1977; Coffee 1986). The key radical-producing step promoting the combustion under most conditions is:

$$N_2O + M = N_2 + O + M \quad . \tag{5}$$

Most of the reactants, H_2 and N_2O, are converted to products, H_2O and N_2, by the fast propagation steps:

$$N_2O + H = OH + N_2 \tag{6}$$

and

$$H_2 + OH = H_2O + H \quad . \tag{7}$$

A small fraction of the N_2O is converted to NO, which is observed at a few mole percent in the burned gases under most conditions. In prior mechanisms, the reaction $N_2O + H = NH + NO$ was believed to be responsible for most of the NO production under rich or stoichiometric conditions. Towards lean conditions, the reaction $N_2O + O = NO + NO$ assumes greater significance for the production of NO.

For our study, a comprehensive chemical mechanism containing over 200 reactions and more than 20 species was initially used to model the detailed chemistry of the H_2/N_2O/Ar flame. Most of the reactions and rate expressions were obtained from the Miller and Bowman mechanism (Miller and Bowman 1989) for gas-phase combustion involving nitrogen compounds. Added to this reaction set were the recombination reactions of NH_x from ammonia chemistry (Dean, Chou, and Stern 1984) and combustion reactions involving NO_2 and N_2O from a recent critical review of the chemical kinetic database for propellant combustion (Tsang and Herron 1991). A few reactions for predicting NO_x formation and destruction were obtained from a paper on HCN/NO_2 combustion (Thorne and Melius 1989). A sensitivity analysis performed on this comprehensive mechanism revealed reactions which were not important for the present experimental conditions. Most of these reactions were eliminated, and as a result, species such as H_2O_2, NH_2, NH_3, N_2H_x, NO_2, NO_3, N_2O_4, HONO, and HNO_3 were removed from the reaction set. The resulting mechanism, listed in Table 1, contains 38 reactions and 14 species and is used to generate the modeling results presented in the following sections. When two reactions involving NNH, whose importance is discussed and discounted in the following sections, are removed, the resulting predictions of the comprehensive mechanism are virtually identical to those from our smaller mechanism.

Table 1. Reaction Mechanism Rate Coefficients in the Form $k = AT^{B}e^{(-C/RT)}$

	Reaction	A[a]	B	C	Reference
1.	$H_2 + O_2 = OH + OH$	1.70E13	0.00	47,780.0	Miller and Bowman 1989
2.	$H_2 + OH = H_2O + H$	2.16E08	1.51	3,430.0	Michael and Sutherland 1988
3.	$H_2 + O = H + OH$	5.06E04	2.67	6,290.0	Miller and Bowman 1989
4.	$H + H + M = H_2 + M$	1.00E18	−1.00	0.0	Miller and Bowman 1989
	H_2/0./ H_2O/0./[b]				
4a.	$H + H + H_2 = H_2 + H_2$	9.20E16	−0.60	0.0	Miller and Bowman 1989
4b.	$H + H + H_2O = H_2 + H_2O$	6.00E19	−1.25	0.0	Miller and Bowman 1989
5.	$H + O_2 = OH + O$	3.52E16	−0.70	17,070.0	Masten et al. 1990
6.	$O_2 + H + M = HO_2 + M$	3.61E17	−0.72	0.0	Miller and Bowman 1989
	O_2/1.0/ N_2/1.3/ H_2O/18.6/ H_2/2.9/[b]				
7.	$O + O + M = O_2 + M$	1.89E13	0.00	−1,788.0	Miller and Bowman 1989
8.	$HO_2 + OH = H_2O + O_2$	7.50E12	0.00	0.0	Miller and Bowman 1989
9.	$HO_2 + H = OH + OH$	1.69E14	0.00	874.0	Tsang and Hampson 1986
10.	$HO_2 + H = H_2 + O_2$	6.63E13	0.00	2,126.0	Tsang and Hampson 1986
11.	$HO_2 + O = OH + O_2$	1.40E13	0.00	1,073.0	Miller and Bowman 1989
12.	$OH + OH = H_2O + O$	6.00E08	1.30	0.0	Miller and Bowman 1989
13.	$H + OH + M = H_2O + M$	1.60E22	−2.00	0.0	Miller and Bowman 1989
	H_2O/5./[b]				
14.	$H + O + M = OH + M$	6.20E16	−0.60	0.0	Miller and Bowman 1989
	H_2O/5./[b]				
15.	$N_2O + H = OH + N_2$	2.53E10	0.0	4,550.0	Marshall et al. 1989
	$N_2O + H = OH + N_2$	2.23E14	0.0	16,750.0	Marshall et al. 1989[c]
16.	$N_2O + M = N_2 + O + M$	7.20E17	−0.73	62,800.0	Tsang and Herron 1991[d]
	NO/0./ N_2O/0./ H_2/0./ O_2/0./ H_2O/0./ N_2/0./ Ar /0./[b]				
16a.	$N_2O + NO = N_2 + O + NO$	7.20E17	−0.73	62,800.0	Tsang and Herron 1991[d]
16b.	$N_2O + H_2 = N_2 + O + H_2$	7.20E17	−0.73	62,800.0	Tsang and Herron 1991[d]
16c.	$N_2O + O_2 = N_2 + O + O_2$	7.20E17	−0.73	62,800.0	Tsang and Herron 1991[d]

[a] Units A=cm-mol-sec-K, C=cal/mole. Low-pressure limits used for unimolecular decomposition and recombination.
[b] Third body efficiencies.
[c] The reaction rate coefficient is computed by the sum of the two expressions.
[d] Third body efficiencies for O_2, Ar, N_2O, N_2 from Baulch, Drysdale, and Horne (1973) and H_2O, H_2 and NO from best estimate.

Table 1. Reaction Mechanism Rate Coefficients in the Form $k = AT^B e^{(-C/RT)}$ (continued)

	Reaction	A	B	C	Reference
16d.	$N_2O + N_2 = N_2 + O + N_2$	7.20E17	-0.73	62,800.0	Tsang and Herron 1991[a]
16e.	$N_2O + N_2O = N_2 + O + N_2O$	3.60E18	-0.73	62,800.0	Tsang and Herron 1991[a]
16f.	$N_2O + H_2O = N_2 + O + H_2O$	3.60E18	-0.73	62,800.0	Tsang and Herron 1991[a]
16g.	$N_2O + Ar = N_2 + O + Ar$	4.82E17	-0.73	62,800.0	Tsang and Herron 1991[a]
17.	$N_2O + O = N_2 + O_2$	1.00E14	0.00	28,000.0	Tsang and Herron 1991
18.	$N_2O + O = NO + NO$	6.60E13	0.00	26,600.0	Tsang and Herron 1991
19.	$N_2O + OH = HO_2 + N_2$	2.00E12	0.00	10,000.0	Miller and Bowman 1989
20.	$NH + NO = N_2O + H$	2.94E14	−0.40	0.0	Miller and Melius, in press[b]
	$NH + NO = N_2O + H$	−2.16E1	−0.23	0.0	Miller and Melius, in press[b]
21.	$NH + NO = N_2 + OH$	2.16E13	−0.23	0.0	Miller and Melius, in press
22.	$NH + O_2 = NO + OH$	7.60E10	0.00	1,530.0	Mertens et al. 1991
23.	$NH + O_2 = HNO + O$	3.89E13	0.00	17,885.0	Mertens et al. 1991
24.	$NH + OH = HNO + H$	2.00E13	0.00	0.0	Miller and Bowman 1989
25.	$NH + OH = N + H_2O$	5.00E11	0.50	2,000.0	Miller and Bowman 1989
26.	$NH + N = N_2 + H$	3.00E13	0.00	0.0	Miller and Bowman 1989
27.	$N + H_2 = NH + H$	1.60E14	0.00	25,140.0	Davidson and Hanson 1990
28.	$NH + O = NO + H$	5.50E13	0.00	0.0	Mertens et al. 1991
29.	$NH + O = N + OH$	3.72E13	0.00	0.0	Mertens et al. 1991
30.	$NH + NH = N_2 + H + H$	5.10E13	0.00	0.0	Mertens et al. 1989
31.	$NH + M = N + H + M$	2.65E14	0.00	75,514.0	Mertens et al. 1989
32.	$HNO + OH = NO + H_2O$	4.80E13	0.00	990.0	Tsang and Herron 1991
33.	$NO + N = N_2 + O$	3.27E12	0.30	0.0	Miller and Bowman 1989
34.	$NO + M = N + O + M$	1.40E15	0.00	148,430.0	Tsang and Herron 1991
35.	$NO + H + M = HNO + M$	9.00E19	−1.30	735.0	Tsang and Herron 1991
36.	$NO + H = N + OH$	1.68E14	0.00	47,570.0	Tsang and Herron 1991
37.	$NO + O = N + O_2$	3.80E09	1.00	41,375.0	Tsang and Herron 1991[c]
38.	$N + N_2O = N_2 + NO$	1.00E13	0.00	19,870.0	Hanson and Salimion 1985

[a] Third body efficiencies for O_2, Ar, N_2O, N_2 from Baulch, Drysdale, and Horne (1973) and H_2O, H_2 and NO from best estimate.

[b] The reaction rate coefficient is computed by the sum of the two expressions.

[c] The expression shown is from Hanson and Salimian (1985), which is recommended in Tsang and Herron (1991). There is a transcription error in Tsang and Herron (1991).

The mechanism was reviewed, and reactions which are important for the present conditions were carefully examined. The rate expression reported by Marshall and coworkers (Marshall, Fontijn, and Melius 1987; Marshall, Ko, and Fontijn 1989) for the reaction $N_2O + H = OH + N_2$ (R15) was incorporated in the mechanism. Those experimental and theoretical studies demonstrated that the reaction rate expression possesses an upward curvature in the Arrhenius plot at low temperature due to quantum mechanical tunneling. Therefore, extrapolating previously reported high temperature expressions to low temperatures could produce inaccurate conclusions. Rate expressions resulting from the recent work of Hanson and coworkers (Mertens et al. 1991; Davidson and Hanson 1990; Mertens et al. 1989) for a number of N, NH, and NO reactions (R22, R23, R27–R31) studied at high temperatures have also been incorporated. In particular, R27 and R33 have also been examined by Koshi et al. (1990), using similar techniques. However, Davidson and Hanson (1990) reported careful calibration of experimental diagnostics, and their error limits are much smaller than those reported by Koshi et al. (1990). Therefore, the rate expression reported by Hanson and coworkers was chosen for R27 and is extrapolated to lower temperatures for the present work. The expression of Miller and Bowman was retained for R33 because it is in good agreement with both the high temperature data (Davidson and Hanson 1990) and results of low temperature critical reviews (DeMore et al. 1987; Atkinson et al. 1989). Other reactions important for our conditions will be discussed in the following sections.

4.2 Comparison Between Model and Experiment. Presented in Figure 2 are the experimentally measured temperatures of a stoichiometric, 20-torr $H_2/N_2O/Ar$ flame. The data are fitted by a sigmoidal function (Miller and Kotlar 1986) and the resulting profile, together with an extrapolated burner surface temperature of 610 K, is used as a fixed input for the flame code. The computed profiles for N_2O, H_2, N_2, H_2O, and Ar generated using the mechanism with hydrogen boundary conditions are compared to the MB/MS experimental profiles in Figure 3. The flame front extends from the burner surface to approximately 15 mm above the burner, as seen by the disappearance of the reactants N_2O and H_2. In the burned gas region, the computed and measured profiles for N_2O deviate slightly, while the H_2 profiles are in agreement. However, near the burner surface, the N_2O profiles compare well, but the computed concentrations for H_2 are much lower than the experimental values. The quartz skimmer may inhibit diffusion near the burner surface which would explain the higher experimental H_2 concentration value. The computed profiles for the products N_2 and H_2O agree with the experimental results over the entire flame zone. The model predicts the absolute concentration values well at both the burner surface and in the burned gas region. However, the model prediction for H_2O in the burned gas region is slightly larger

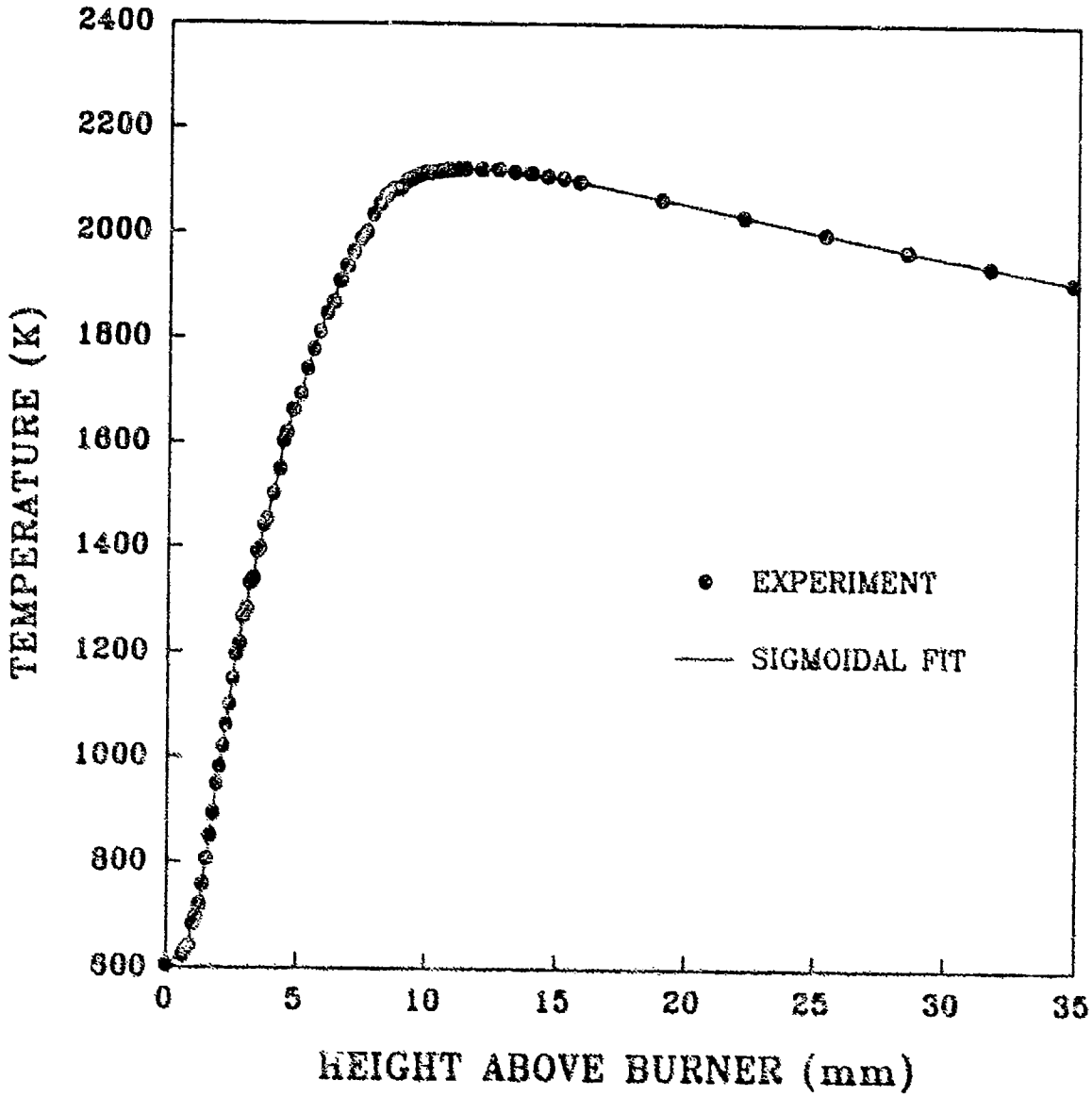

Figure 2. Temperature profile of a stoichiometric, 20 torr $H_2/N_2O/Ar$ flame measured with a coated Pt/Pt-Rh(10%) thermocouple. The data are fit to a sigmoidal function which is used as a fixed input to the flame code.

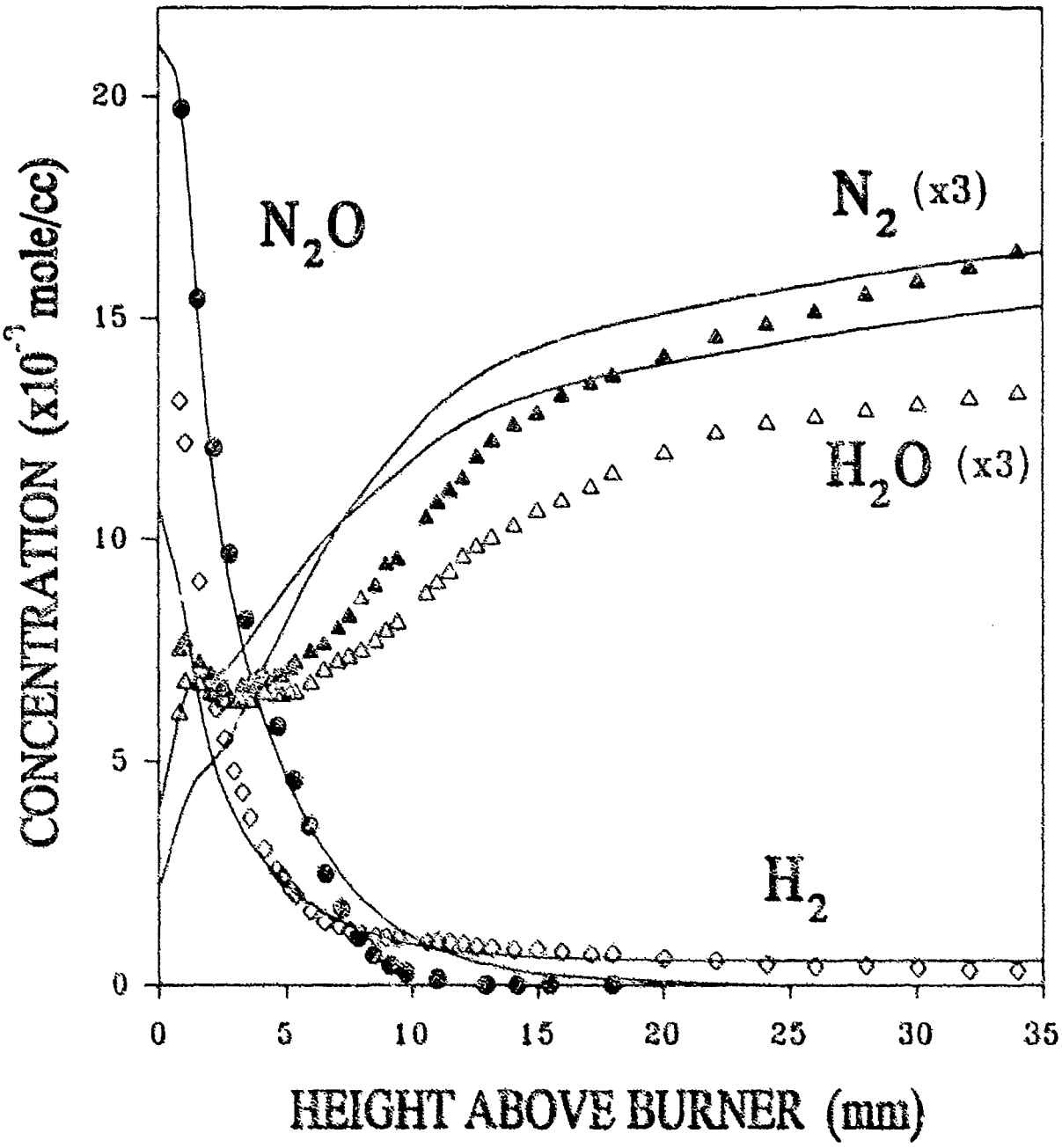

Figure 3. Measured and computed majority species profiles. The absolute values for all the species were measured.

than the experimental value which may result from difficulties in the calibration of the MB/MS H_2O signal. Overall, the agreement between the measured and predicted majority species profiles is acceptable.

Presented in Figure 4 are the calculated and experimental concentration profiles for NO and NH. The absolute value of the predicted NO concentration agrees well with the experimental results in the postflame region, even though there may be a slow reaction consuming NO in this region missing in the model. The NH profile is normalized to the model concentration profile since absolute measurements were not obtained for NH. Although the model and experimental shapes of the NH profiles are similar, the modeled NH profile is shifted approximately 2 mm further away from the burner surface than the experimentally measured one. It is difficult to determine whether this is the result of a slight perturbation induced by the MB/MS technique or inaccuracies in the mechanism.

Experimental profiles measured using both MB/MS and LIF for the OH radical are shown in Figure 5 along with the model results. Absolute values were not determined in either experiment, therefore, the experimental profiles are normalized to the calculated concentrations. The relative profiles for the LIF experimental results agree very well with the model. The profile for the MB/MS agrees reasonably with the model profile except near the burner surface (3 to 6 mm) where the MB/MS shows a reduced concentration at 4 mm. This feature is probably an artifact of the MB/MS technique since the LIF profiles do not show this anomaly. The LIF technique is less intrusive and care has been taken to avoid possible perturbing effects such as saturation, temperature variation, and quenching.

Figure 6 shows the experimentally measured profiles of the radical species O and H normalized to model profiles. The O-atom profile shown is an average of two scans recorded using an electron energy of 15.3 ± 0.1 eV, just below the threshold for forming O^+ from N_2O (Collin and Lossing 1958). Overall, the agreement between experiment and model profiles is good considering the rather poor signal-to-noise in the experiment. In the case of the H-atom profiles, agreement between the experiment and model is fair.

Presented in Figure 7 are the calculated profiles of O_2 and HO_2. Various rate coefficients for reaction R19 were used since the exact expression is not well established. The experimental profile for O_2 is predicted reasonably well for two of the model profiles and will be discussed later. The HO_2 radical,

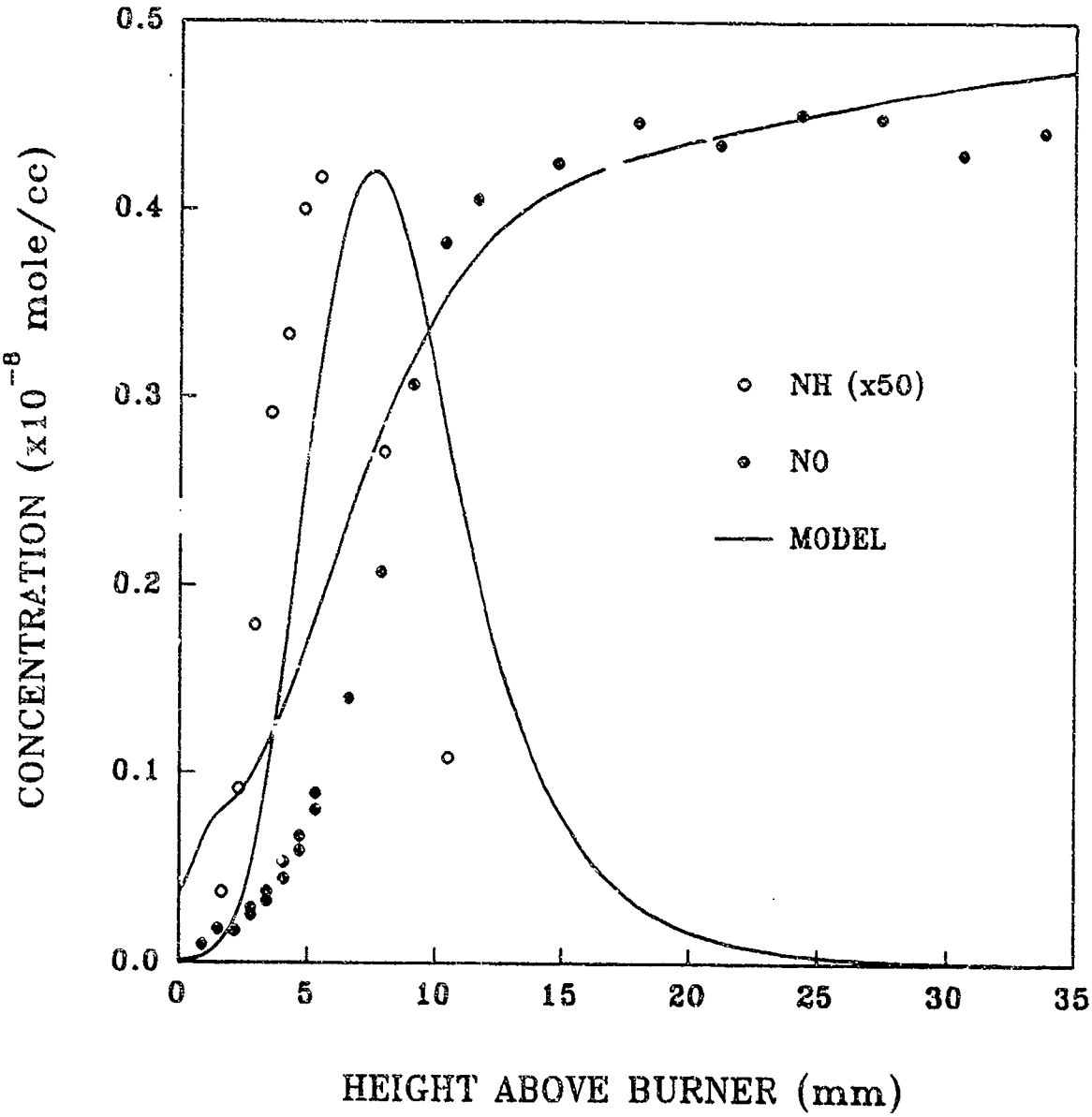

Figure 4. Measured and computed profiles of NO and NH. The absolute value of the NO was measured. The measured NH profile was normalized to the computed profile.

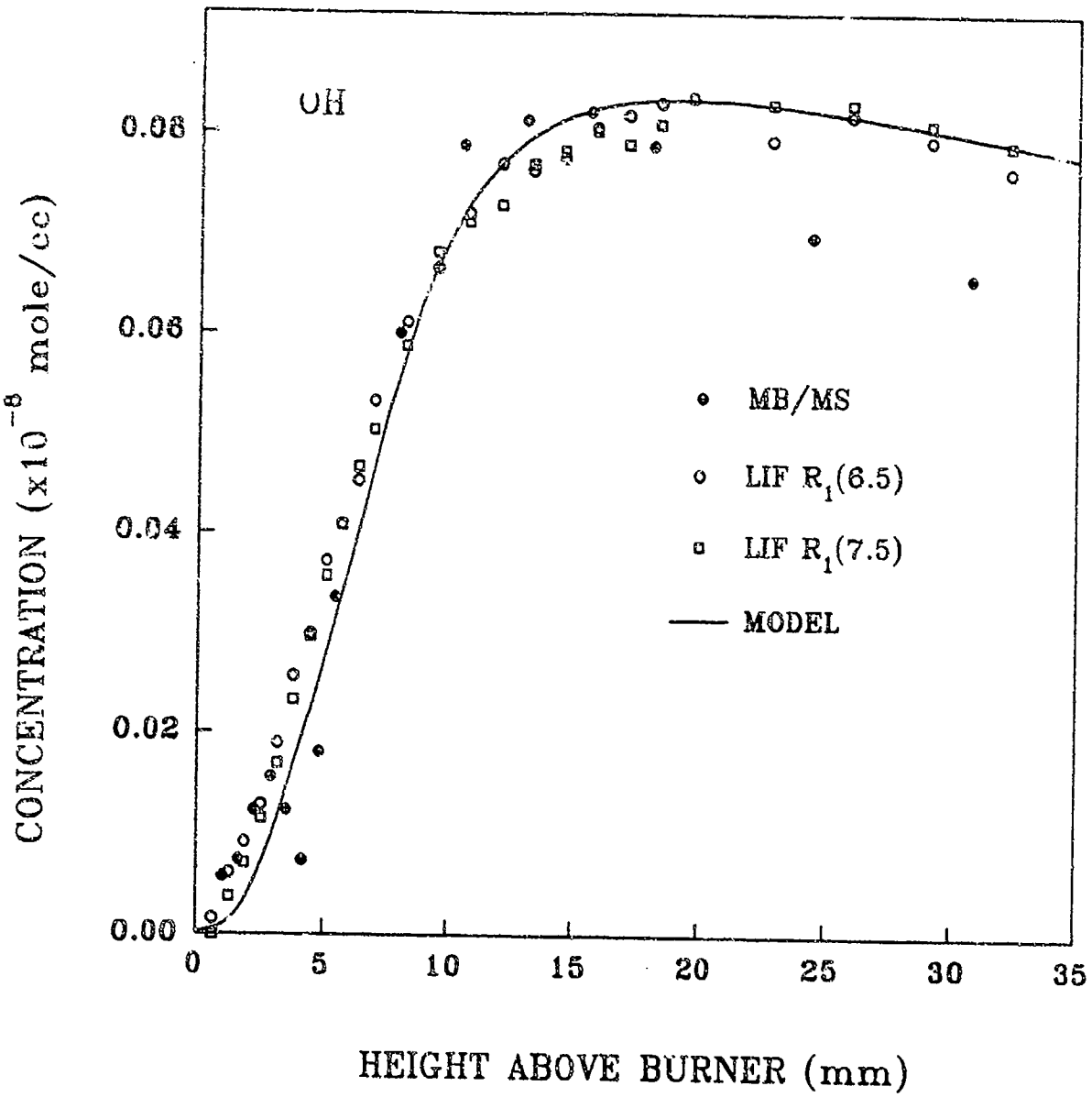

Figure 5. Measured and computed profiles of OH. The measured profiles were normalized to the computed profile.

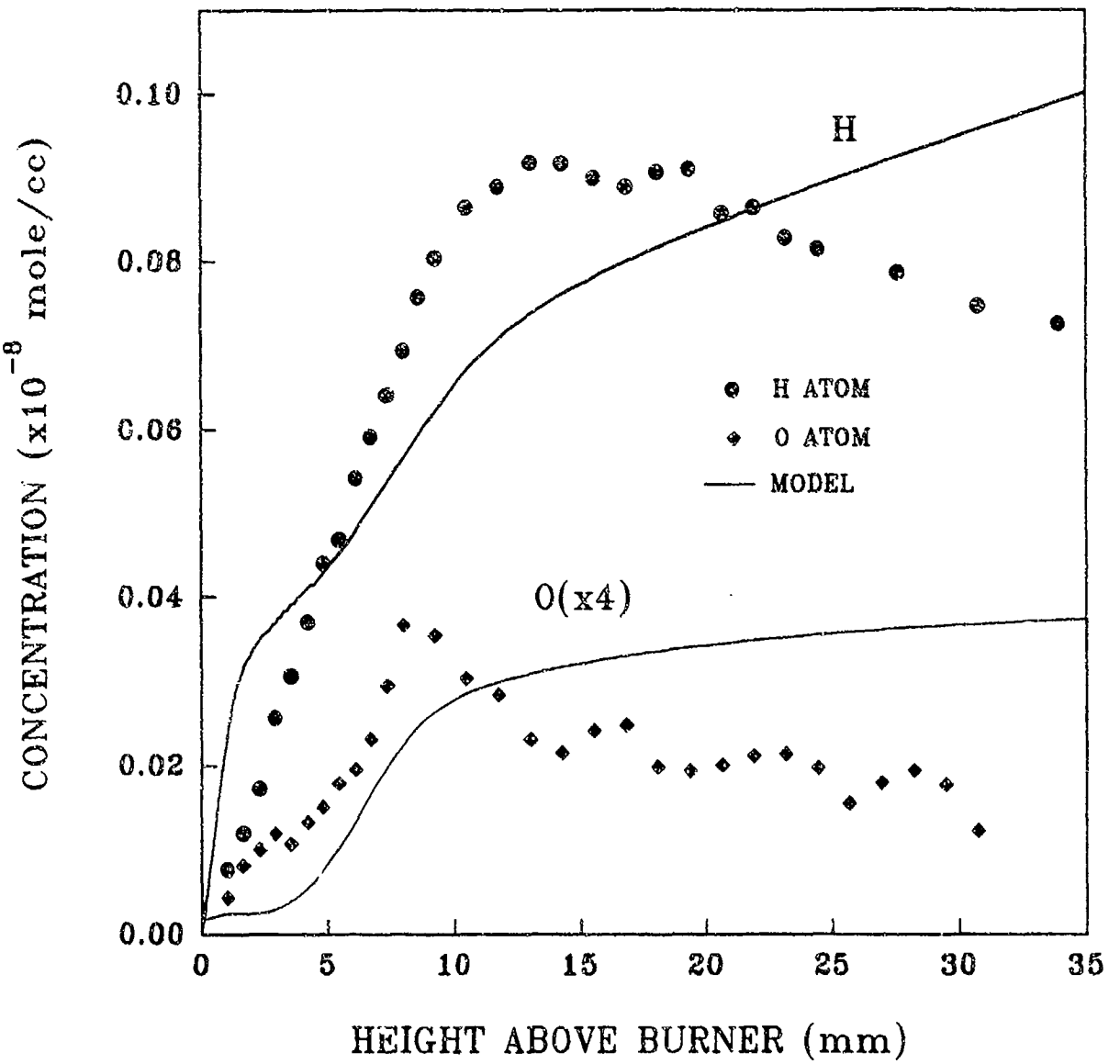

Figure 6. Measured and computed profiles of O and H atoms. The measured profiles were normalized to the computed profiles.

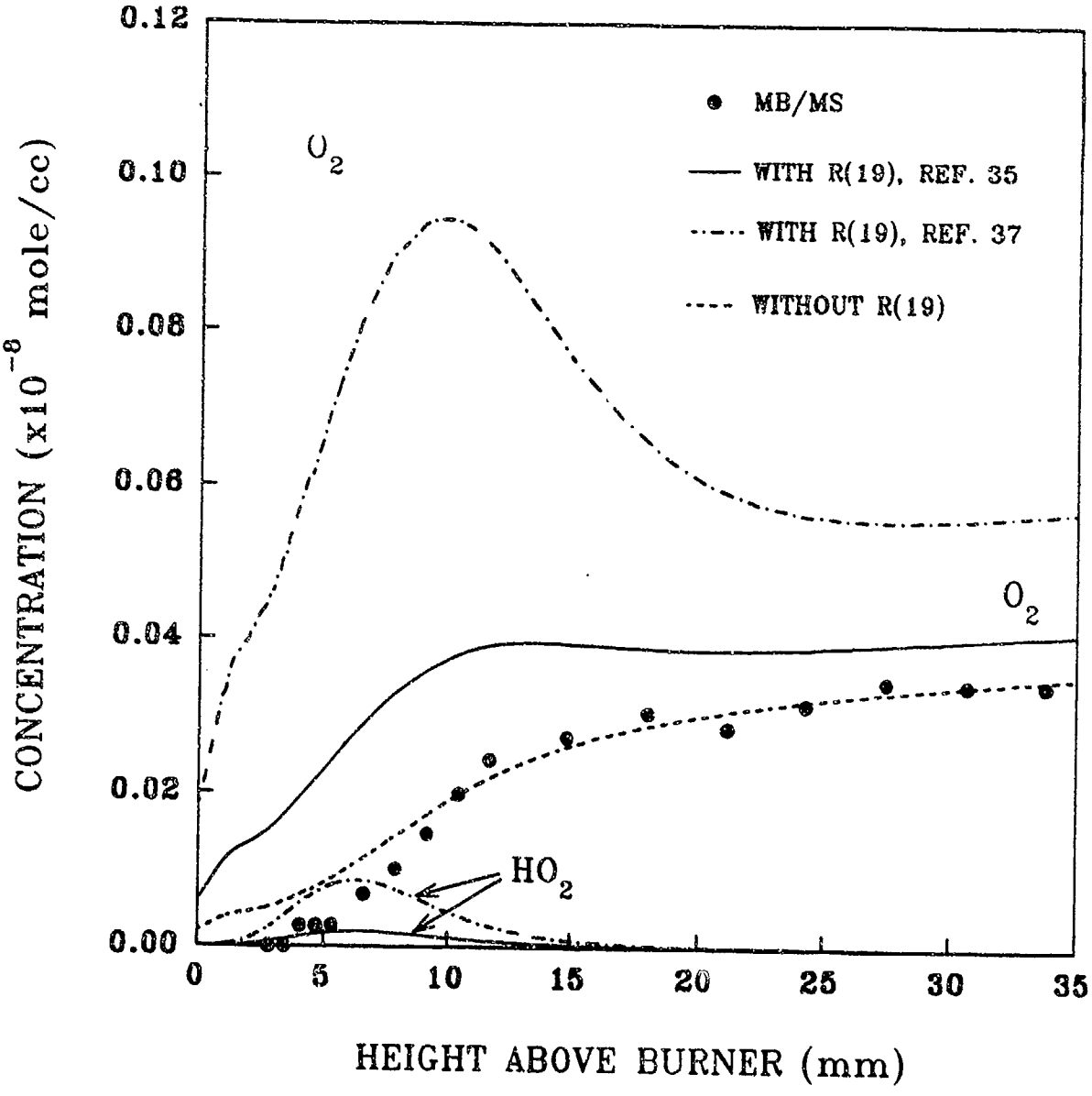

Figure 7. Measured and computed profiles of O_2 and computed profiles of HO_2. The absolute value for O_2 was measured. The rate coefficient for $N_2O + OH = HO_2 + N_2$ (R19) was changed from the mechanism (solid line) to the critical review's (Tsang and Herron 1991) upper limit (dotted line) and zero, omitted from the mechanism (dashed line).

however, could not be detected under our experimental conditions. Unfortunately, firm conclusions regarding the chemistry cannot be drawn since the lower limit of detection for this species is not known.

The effects of temperature on the predicted species concentration profiles were also examined since the experimental temperature data was used as a fixed input to the flame code calculations. A ±5% difference in the temperature profile, twice the experimental uncertainty, results in a ±10–15% difference in the computed NO and O_2 burned gas concentrations, a ±20–30% difference in the H, O, and OH concentrations, and approximately ±5% difference in the NH, N, HNO, and HO_2 trace intermediates. The flame zone width, as determined from the computed species profiles, changes only slightly compared to the observed width, approximately ±0.5–1 mm. Thus, only the computed H, O, and OH profiles have much dependence on temperature. The significance of these changes cannot be examined since the absolute concentrations of these species were not measured. Even the 20–30% changes are not large compared to typical error limits in measured absolute radical concentrations.

4.3 Flame Structure Analysis.

4.3.1 Overview of the Nitrogen Chemistry. Analysis of the postprocessor results yields reaction pathway diagrams constructed using the mechanism in Table 1. The reaction pathway diagram depicting the nitrogen chemistry occurring at approximately 7 mm above the burner surface is shown in Figure 8. This point is halfway through the flame zone and is calculated to be the position of maximum chemical heat release in the flame. Qualitatively this diagram is not expected to change much at various heights in the flame zone due to the single stage nature of the flame. The numbers in parentheses are the relative rates of the various reactions, normalized to 100 for the reaction $N_2O + H = OH + N_2$ (R15) representing the fastest step consuming N_2O. The initiation step, $N_2O + M = N_2 + O + M$ (R16), and the reaction $N_2O + OH = HO_2 + N_2$ (R19) are also important reactions in the direct conversion of N_2O to N_2. According to the diagram, prediction of the concentration of NO is quite complex because a portion of the NH formed by $N_2O + H = NH + NO$ (-R20) reacts with H or OH to form N atoms, which in turn primarily react with NO to form N_2. However, there are a number of other competing pathways involving NH and N atoms which may result in the formation of either additional NO or N_2. Surprisingly, most of the rate coefficients for the reactions which affect the computed NO concentration have been carefully studied.

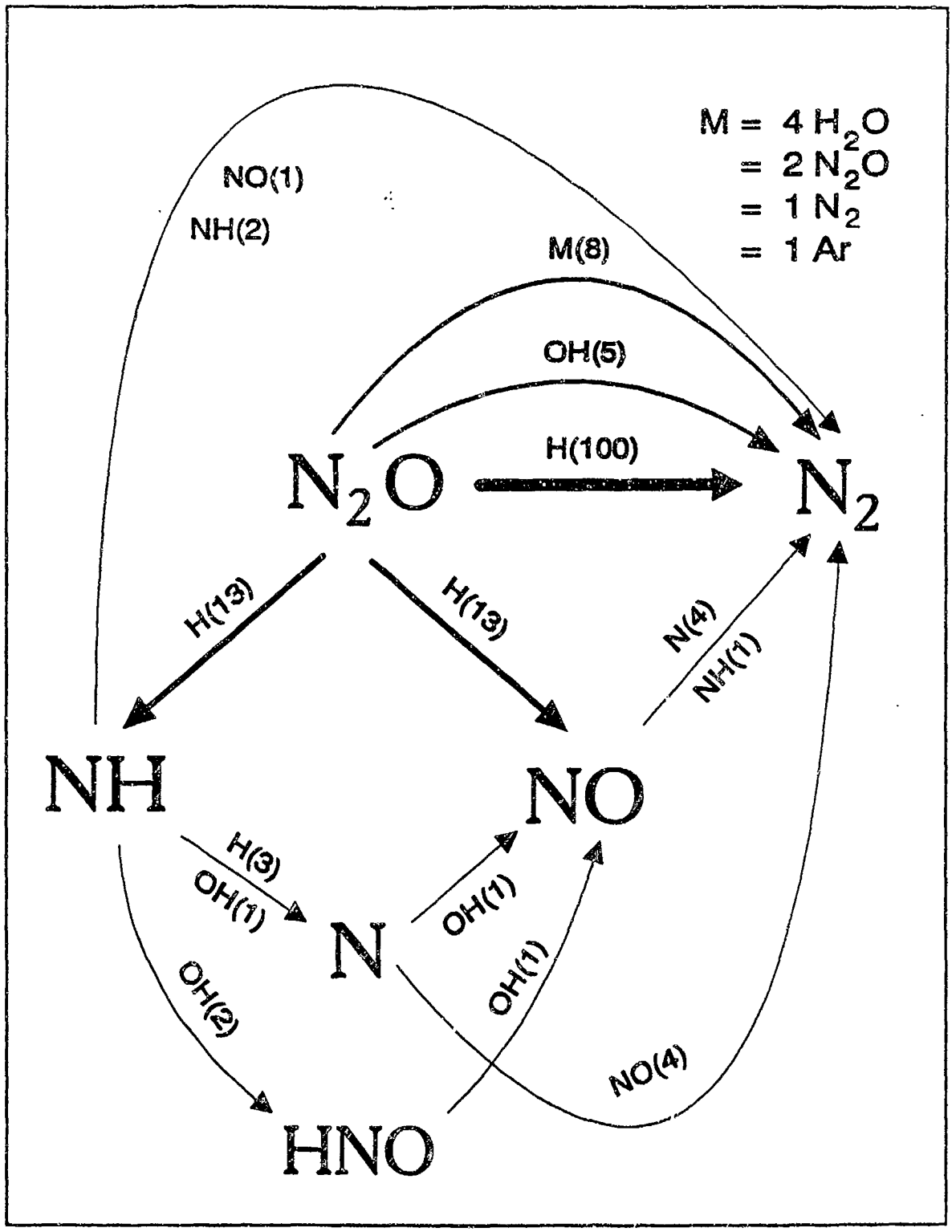

Figure 8. Reaction pathway diagram for the nitrogen chemistry occurring in the stoichiometric $H_2/N_2O/Ar$ flame. The diagram depicts the most important reactions at ~7 mm above the burner surface, the point of maximum heat release rate in the flame. The numbers in parentheses are relative rates of the various reactions scaled to 100 for $N_2O + H = OH + N_2$ (R15). The legend depicts the breakdown of the reaction $N_2O + M = N_2 + O + M$ (R16) into contributions from the various colliders.

Information concerning the overall combustion rate can be found by examining sensitivities of a major species. For example, the sensitivity plot for N_2O in Figure 9 was calculated using the reaction set listed in Table 1 and, as expected, the radical-producing reaction R16 has the largest effect on the N_2O concentration. Sensitivities of the propagating steps R2 and R15 are also large.

As mentioned previously, a sensitivity analysis was also run on the comprehensive mechanism (>200 reactions). Surprisingly, the overall combustion rate was found to be *highly* sensitive to the reactions $N_2O + H = NNH + O$ (R39) and $NNH + M = N_2 + H + M$ (R40). The overall combustion rate was sensitive to these two reactions since the sequence is chain branching and produces two radicals. The sensitivity coefficient for R39 had approximately the same magnitude as that for the initiation step, $N_2O + M$ (R16). Additionally, the rate of radical pool buildup by these two paths was predicted to be nearly equal. The rate expression for –R39, taken from the Miller and Bowman mechanism (Miller and Bowman 1989), is an upper limit estimate (Miller 1993) (1.00×10^{14}cm^3/mol-s). R40 was taken from Miller et al. (1983) and collider efficiencies for R40 were assumed to be identical to R6. When these reactions were included in the mechanism the predicted flame speed increased and the predicted shapes of the species profiles are compressed slightly (10–15%) towards the burner. The absolute concentrations in the burned gas region for all species change only slightly (<5–10%) except for the H, O, and OH concentrations which increase by ~30–75%. Unfortunately, it is not possible to determine whether these reactions are important based on the present experimental profiles since both sets of predictions, with or without R39 and R40, agree within error limits of the experimental results.

For the reaction of H with N_2O, Marshall and coworkers (Marshall, Fontijn, and Melius 1987; Marshall, Ko, and Fontijn 1989) present upper limit estimates based on thermodynamic arguments for the rate constant expression for the products NH + NO (–R20) and for the branching ratio to NNH + O (R39) at 2,000 K. The activation energy for R39 is taken to be no smaller than the endothermicity of the channel. Following their methods, the upper limit rate expression ($k = 5 \times 10^{14} e^{(-45{,}000/RT)}$cm^3/mol-s) for the NNH + O channel is approximately a factor of 30 lower than what is obtained by reversing the expression of Miller and Bowman in the temperature range of interest. When this smaller rate coefficient is used in the mechanism, the reaction has little significance, even for higher temperature conditions (e.g., $\phi = 1.0$, atmospheric pressure free flame, no diluent). The apparent inconsistency upon reversing rate coefficients is possibly due, in part, to uncertain thermodynamic data for NNH. Therefore, reactions R39 and R40 were excluded from our mechanism.

R2	$H_2 + OH = H_2O + H$	R20	$NH + NO = N_2O + H$
R3	$H_2 + O = H + OH$	R27	$N + H_2 = NH + H$
R15	$N_2O + H = OH + N_2$	R33	$NO + N = N_2 + O$
R16	$N_2O + M = N_2 + O + M$	R36	$NO + H = N + OH$

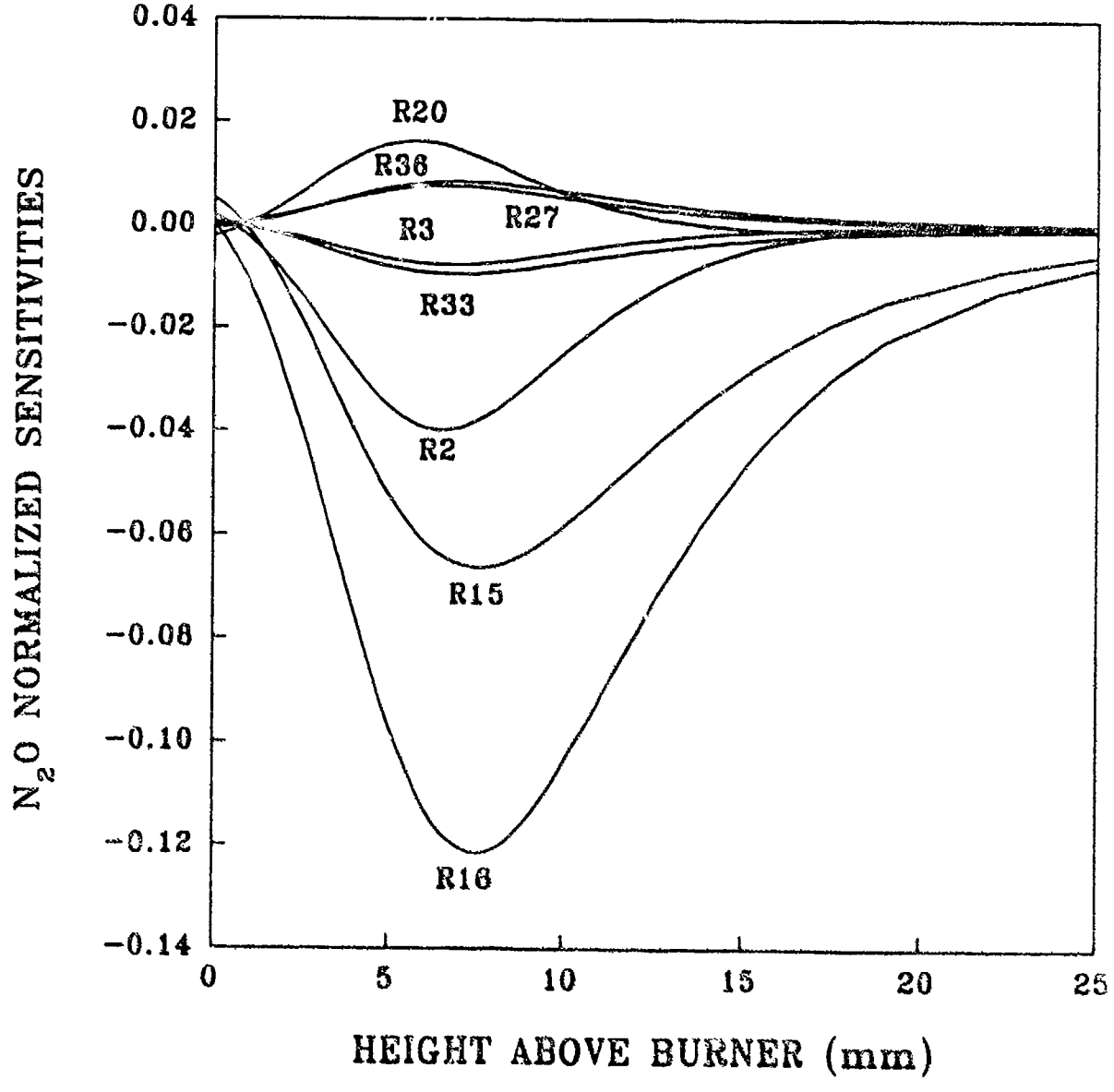

Figure 9. Sensitivity plot for N_2O in the stoichiometric $H_2/N_2O/Ar$ flame.

4.3.2 Conversion of N_2O to N_2. As discussed earlier, the reaction $N_2O + H = OH + N_2$ (R15) plays the prominent role in the direct conversion of N_2O to N_2. The remainder of the direct conversion results primarily from reactions $N_2O + OH = HO_2 + N_2$ (R19) and $N_2O + M = N_2 + O + M$ (R16). It has been suggested by a number of researchers (Miller and Bowman 1989; Schoffield, Vandooren, and Van Tiggelen 1986; Tsang and Herron 1991; Yetter et al. 1991) that R19 may be important in several systems; however, its rate constant is poorly established. Yetter et al. (1991) found it necessary to include this reaction to model their H_2/N_2O flow system experiments at intermediate temperatures (925–1,073 K). Under these conditions, the effects of this reaction on the overall combustion are inhibitive, presumably because HO_2 is a slowly reacting radical compared to H, O, and OH, and also because formation of HO_2 results in removal of radicals from the system by $HO_2 + H = H_2 + O_2$ (R10). Use of the upper limit rate expression for R19 from the critical review of Tsang and Herron (1991) resulted in a strong inhibiting effect which did not properly model the flow system results. Reasonable agreement was found when using the expression of Miller and Bowman (1989), a factor of 3–4 smaller. Miller and Bowman derived their expression to help explain concentration profiles measured in an NH_3/O_2 flame by Bian, Vandooren, and Van Tiggelen (1986). Using their mechanism, Miller and Bowman predicted that N_2O in that flame is formed primarily by $NH + NO = N_2O + H$ (R20) and consumed by R15 and R19. At that time, the rate constant of R20 at high temperature was poorly established. Miller and Bowman stated that if subsequent work resulted in an increase of this rate constant, one possible way to compensate for the increase in N_2O concentration without affecting seriously any of the other predicted species profiles would be to increase the rate coefficient of R19. As will be discussed later, a slight increase at the high temperature end of the rate expression for R20 is herein recommended. Unfortunately, this creates a dilemma because the present experimental results would be best explained if the rate coefficient for R19 were *smaller than* that from the Miller and Bowman expression.

The rate expression listed in Table 1 for R19 is from Miller and Bowman (1989). Examining the sensitivity diagram for O_2, shown in Figure 10, reveals that the O_2 concentration is sensitive to R19 and to the branching ratio between R9 and R10 since R10 forms O_2 directly. All of the measured species exhibit little or no sensitivity to R19 except for O_2. Figure 7 shows calculated O_2 and HO_2 profiles employing different rate expressions for R19. The solid curve is generated using the mechanism in Table 1, while the other two curves were generated by changing the rate expression to: 1) upper limit as recommended by Tsang and Herron (1991); and 2) zero (that is, the reaction is not included). If the upper limit rate expression is used, then the O_2 sensitivity to this reaction increases, as expected. Also, N_2O sensitivity to R9 and R10 becomes important, and inhibiting effects are noticeable. As seen in Figure 7,

R2	$H_2 + OH = H_2O + H$	R16	$N_2O + M = N_2 + O + M$
R9	$HO_2 + H = OH + OH$	R19	$N_2O + OH = N_2 + HO_2$
R10	$HO_2 + H = H_2 + O_2$	R20	$NH + NO = N_2O + H$
R15	$N_2O + H = OH + N_2$	R24	$NH + OH = HNO + H$

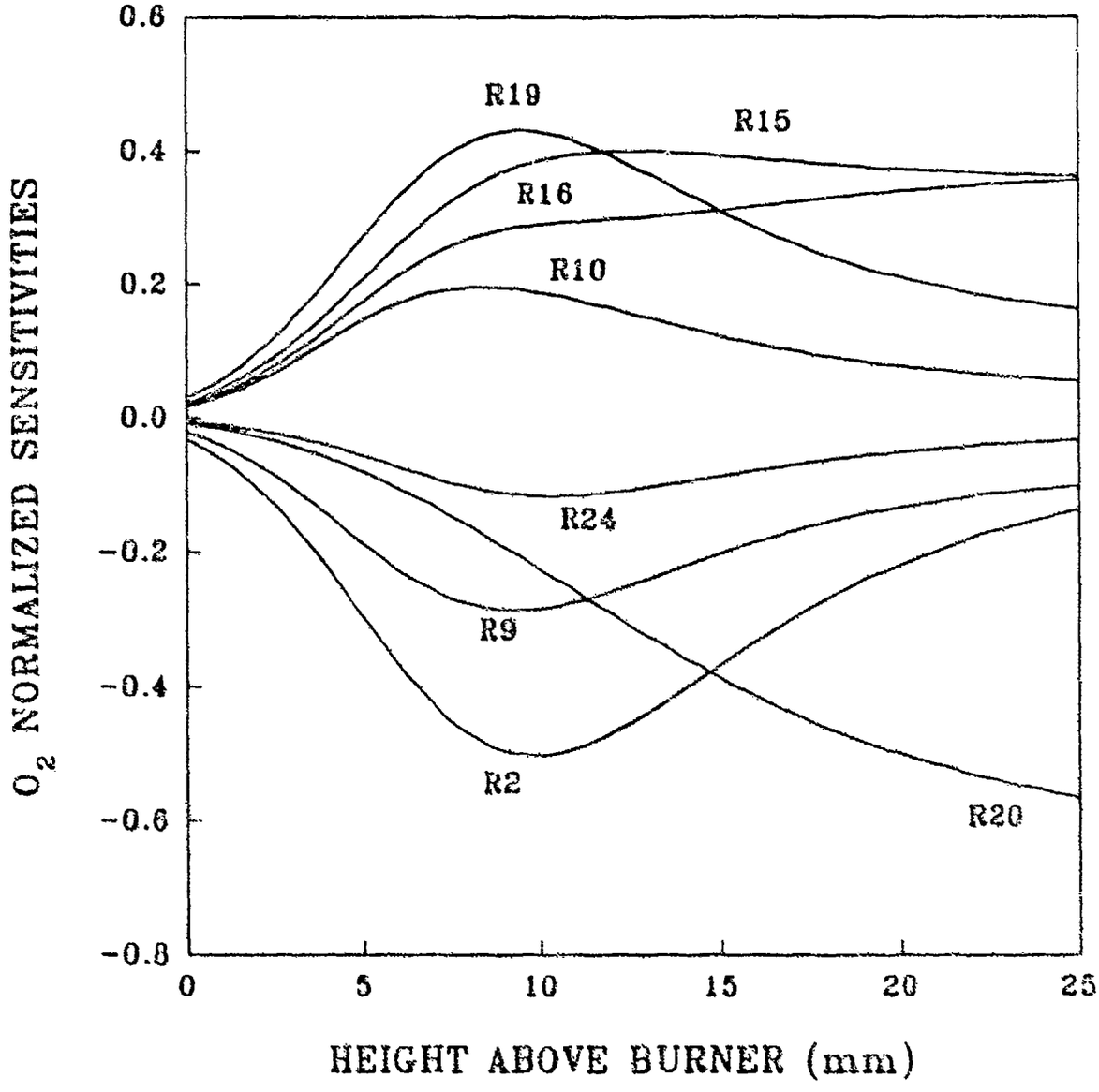

Figure 10. Sensitivity plot for O_2 in the stoichiometric $H_2/N_2O/Ar$ flame.

a large peak at 10 mm is noticed in the O_2 profile when the upper limit rate expression is used. The experimental profile obtained with the MB/MS clearly does not show a peak. Adequate agreement between the model and experiment in this region of the flame can only occur while still maintaining the large rate coefficient for R19 if several of the reactions to which the O_2 profile is most sensitive are changed *simultaneously* to the limits of their uncertainties. Such a drastic alteration of the mechanism seems unreasonable even though the other calculated profiles are only slightly affected. If reaction R19 is excluded from the mechanism, then the predicted and experimental O_2 profiles agree well. The above results indicate that the Miller and Bowman rate expression for R19 is more consistent with our experimental conditions than the higher critical review value. Moreover, leaving the reaction out or lowering the rate constant further yields results which are more consistent with our experimental data. However, without any justification for lowering the expression for R19, our recommendation is to retain it in the mechanism. Further investigation of this reaction is clearly needed.

The N_2O concentration and, hence, overall combustion, is highly sensitive to the initiation step, $N_2O + M = N_2 + O + M$ (R16), as seen in Figure 9. To further examine this reaction, the effects of individual collision partners were included in the reaction mechanism (R16a–R16g) in order to assess which colliders are most important. The third body efficiencies for O_2, Ar, N_2O, and N_2 are from a critical review (Baulch, Drysdale, and Horne 1973) and the values for H_2O, H_2, and NO are estimated. Only the third body efficiency for Ar is precisely known. As seen on the reaction pathway diagram in Figure 8, the rates of reactions for H_2O and N_2O as collision partners are the most significant. H_2O and N_2O have the largest effect on the N_2O concentration as indicated in the N_2O sensitivity plot for the $N_2O + M$ reaction for different colliders, shown in Figure 11. The reactant H_2 as a collider does not appear important possibly due to the low-pressure conditions which enhance the diffusion of light species, thus reducing the concentration of H_2 near the burner surface. However, at higher pressures diffusion is not so large an effect and H_2 as a collider may become more important. Also, the efficiency for H_2 as a collider is assumed to be small, as is frequently observed for many reactions. This assumption contributes to the prediction of low sensitivity for the reaction.

4.3.3 Conversion of N_2O to NO. Formation of a few percent of NO has an important inhibiting effect on the overall rate of combustion because less heat is released when it is formed compared to the more typical products, N_2 and H_2O. Presented in Table 2 is a comparison of the measured burned gas composition for the present flame at 25 mm above the burner surface with that calculated with the flame code. Also presented in Table 2 are the species concentrations obtained from a NASA-Lewis chemical

R16 $N_2O + M = N_2 + O + M$

M = H_2O, N_2O, N_2, Ar, H_2, NO, O_2

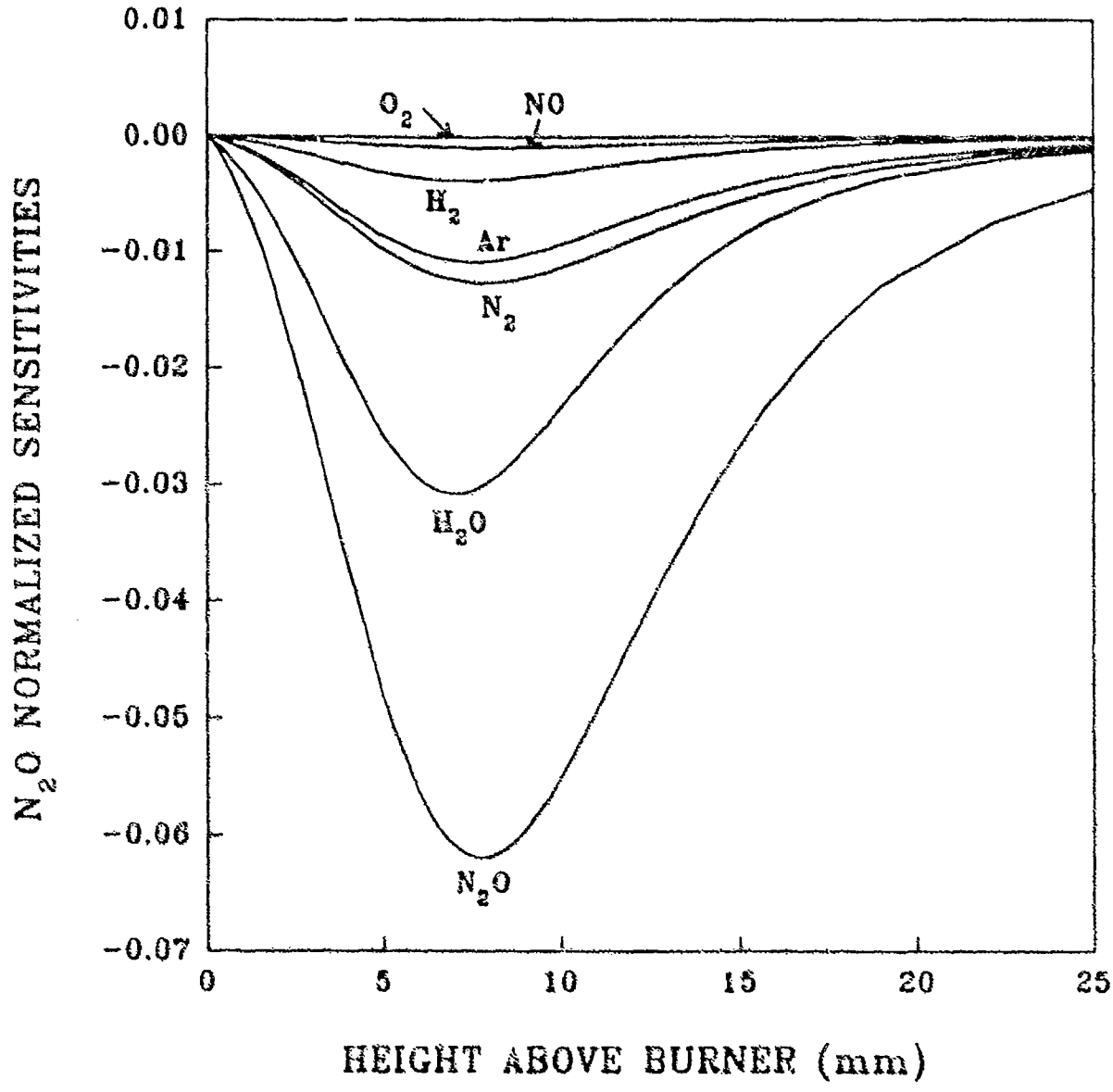

Figure 11. Sensitivity plot of N_2O to the reaction $N_2O + M = N_2 + O + M$ (R16) for individual colliders in the stoichiometric $H_2/N_2O/Ar$ flame.

Table 2. Experimental and Calculated Major Species Concentrations in the Post Flame Region[a]: Units are in mol/cm^3 ($\times 10^{-8}$)

Species	Experiment	Premix Model	Nasa-Lewis (Equilibrium)
H_2	0.45	0.546	0.154
N_2O	0.00	0.016	0.000
N_2	5.4	5.20	5.53
H_2O	4.4	4.81	5.35
NO	0.45	0.450	0.011
O_2	0.032	0.038	0.060

[a] Height above burner ~25 mm and temperature ~2,000 K.

equilibrium code (Svehla and McBride 1973) calculation using a temperature of 2,000 K. This temperature corresponds to a height of about 25 mm in the flame. Notice that the measured concentrations and those calculated with the flame code agree reasonably well. However, both the measured and predicted concentrations of H_2 and NO are considerably larger than the equilibrium concentrations. Careful inspection of the table reveals that H_2O and O_2 are predicted by the flame model to be slightly *lower* than equilibrium. This result is best seen by comparing the calculated concentrations since the difference is much smaller than the precision of the measurements. Using the predicted concentrations from the flame code and the measured temperature of 2,000 K as input parameters to the equilibrium code, the calculated adiabatic flame temperature of this mixture is found to be approximately 2,200 K, 200 K higher. As further evidence of the importance of the NO formation, flame speeds were calculated for the free flame corresponding to our conditions. (Note, however, there are no heat losses in the energy equation.) For the mechanism given in Table 1, the calculated flame speed is 179.0 cm/s. When all of the NO reactions are removed, the calculated flame speed is 228.2 cm/s. Thus, one sees that the formation of NO is not only of significance in pollutant formation, but can also be very important in determining the gross behavior of N_2O oxidized combustion.

A sensitivity plot for NO obtained using the mechanism in Table 1 is shown in Figure 12. The reaction $N_2O + H = NH + NO$ (−R20) is highly sensitive in the burned gas region and is the major source of NO production at the present conditions. Until recently, the rate expression was not well established from the few high-temperature measurements available since all of these involved complex mechanism

R2 $H_2 + OH = H_2O + H$

R15 $N_2O + H = OH + N_2$

R16 $N_2O + M = N_2 + O + M$

R20 $NH + NO = N_2O + H$

R24 $NH + OH = HNO + H$

R33 $NO + N = N_2 + O$

R36 $NO + H = N + OH$

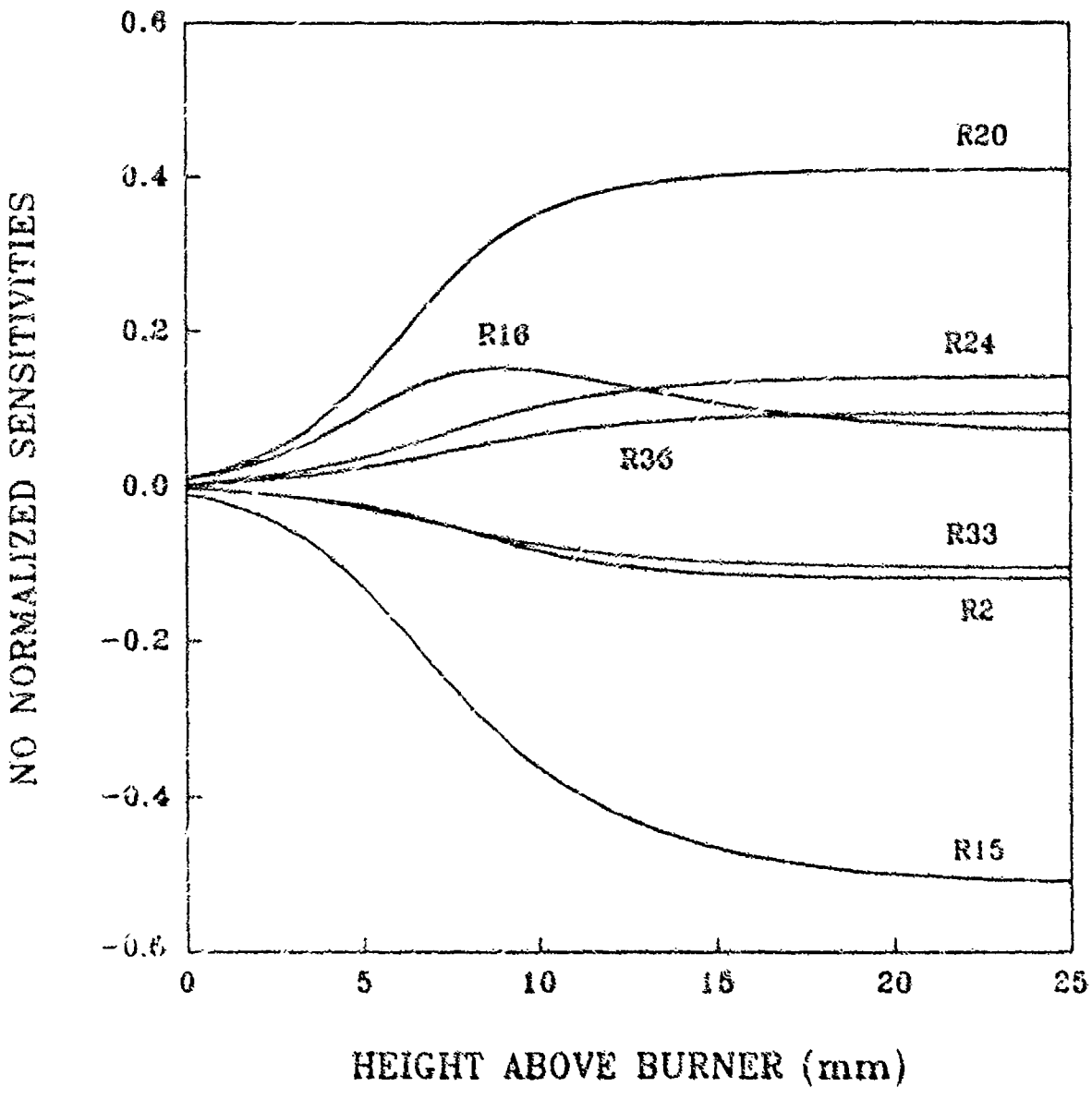

Figure 12. Sensitivity plot for NO in the stoichiometric $H_2/N_2O/Ar$ flame.

fits. Consequently, a wide range of rate expressions has been used to model N_2O combustion (Cattolica, Smooke, and Dean 1982; Coffee 1986; Miller and Bowman 1989; Miller et al. 1983). Two of the rate expressions used by Miller and coworkers (Miller and Bowman 1989; Miller et al. 1983) are considerably larger than the others in the temperature range of interest. Initial attempts to model the present experiment using the expression of Miller and Bowman (1989) resulted in an underprediction of the NO mole fraction and an overprediction of O_2 in the burned gases by approximately 25% each. The computed O_2 concentration in the burned gas region has a strong negative sensitivity for R20 (see Figure 10) because of NH production followed by subsequent reactions R22 and R23 and the sequence –R27 followed by –R37. Using the earlier expression of Miller et al. (1983) for R20, which is slightly larger at high temperatures, brought the production of NO and O_2 to within 5% of the experimental values. A recent transition state theory calculation by Miller and Melius (1992) has led to a theoretical expression which is similar to that of Miller et al. (1983) and is our recommendation. Also, a recent experimental and modeling study by Martin and Brown (1990a, 1990b) on CH_4/air and H_2/O_2/Ar flames doped with N_2O, NO, or NH_3 strongly supports our recommendation. In their work, detailed rate and sensitivity analyses were performed for the N_2O in the two flames containing NH_3. It was shown that the N_2O in these flames is formed almost exclusively by R20 and destroyed primarily by R15 (R19 was also considered). By examining the sensitivity coefficients presented in that work for N_2O, one can show that if a much smaller rate coefficient, say a factor of 5–10, were to be used for R20, the N_2O concentrations would be severely underpredicted. Thus, it appears the rate of –R20 is much larger than that used by Cattolica, Smooke, and Dean (1982) and Coffee (1986).

The reaction of NH with NO has been the subject of a number of theoretical and experimental investigations (Gorden, Mulac, and Nangia 1971; Hansen et al. 1976; Harrison, Whyte, and Phillips 1986; Yamasaki et al. 1991; Vandooren et al. 1991; Mertens et al. 1991; Yokoyama, Sakane, and Fueno 1991; Durant and Rohlfing 1993; Michaud, Westmoreland, and Feitelburg, in press; Bozzelli and Dean 1993; Fueno, Fukuda, and Yokoyama 1988; Harrison and MacIagan 1990), most of these very recent, which center on the rate of reaction at various temperatures and the channels for product formation. There is remarkably good agreement among the low-temperature determinations (Gordon, Mulac, and Nangia 1971; Hansen et al. 1976; Harrison, Whyte, and Phillips 1986; Yamasaki et al. 1991), so that the overall rate coefficient is near collisional with a value of approximately 3×10^{13} cm^3/mol-s. This result is invariant at a pressure range from at least 300 torr (Gordon, Mulac, and Nangia 1971; Hansen et al. 1976; Harrison, Whyte, and Phillips 1986; Yamasaki et al. 1991), and using a wide array of carrier gases (cf. Harrison, Whyte, and Phillips 1986). At higher temperatures the agreement between the experiments is fair, but not

as good (Vandooren et al. 1991; Mertens et al. 1991; Yokoyama, Sakane, and Fueno 1991). Of experiments wherein the branching ratios were measured, three favor the N_2O + H channel (Mertens et al. 1991; Yokoyama, Sakane, and Fueno 1991; Durant and Rohlfing 1993) in agreement with our work, and two favor the N_2 + OH channel (Yamasaki et al. 1991; Vandooren et al. 1991). The work of Vandoren et al. (1991) was an interpretation of an NH_3 flame experiment wherein the results are highly dependent upon absolute concentrations of several of the radical species which could not be measured better than to within a factor of two. The resulting rate coefficients must have very large error limits, quite possibly large enough to be compatible with N_2O actually being the preferred product. The total of the two channels is, however, in fair agreement with other high-temperature measurements. Yamasaki et al. (1991) concluded that *only* the N_2 + OH products are formed. It is not clear why this disagrees so strongly with the other results. In addition to these experimental results, there have been several theoretical calculations (Miller and Melius 1992; Durant and Rohlfing 1993; Michaud, Westmoreland, and Feitelburg, in press; Bozzelli 1993), all of which conclude that the N_2O channel is strongly preferred. The main reason for this involves the energetics of the reaction's potential surfaces. All of the surface studies on the reaction (Miller and Melius 1992; Durant and Rohlfing 1993; Fueno, Fukuda, and Yokoyama 1988; Harrison and MacIagan 1990; Walch 1993) agree, qualitatively, that the reaction starting from NH + NO proceeds through a cis HNNO intermediate in a $^2A'$ state which connects adiabatically with the two product channels. The barrier to H atom transfer, leading to NNOH which rapidly dissociates to N_2 + OH, is approximately 6 kcal/mol higher than that for simple H atom elimination. The reaction therefore strongly favors the H + N_2O channel. Walch (1993) has carefully examined the NH + NO entrance and found that there are barriers of a few kcal/mol in the $^2A'$ surface, but none in the other symmetry allowed surface, $^2A''$. The $^2A''$ surface leads to an excited state of HNNO which could stabilize, but which cannot further react to products. In contrast, the low-temperature study of Harrison, Whyte, and Phillips (1986) indicates that there is no appreciable barrier to the overall reaction. The observed near-collisional rate at low temperature also strongly supports this conclusion. However, the fact that the overall rate exhibits no pressure dependence shows that stabilized HNNO cannot be the major product. If Walch (1993) is correct concerning the entrance channel barriers, these results suggest that the favored reaction path involves approach of NH and NO on one of the $^2A''$ surfaces followed by a crossing to the cis $^2A'$ surface on which the final products can be reached. Corroborative studies of these entrance channel characteristics and the crossing probability would be most interesting.

The NO sensitivity plot in Figure 12 indicates that several reactions involving the NH and HNO radicals and N atoms have a more modest effect on NO formation. This result may be understood by considering the reaction pathway diagram in Figure 8. Some of the NH radicals formed by –R20 are converted to N atoms by reactions with H or OH. The N atoms primarily react with NO to form N_2, although some form additional NO by a reaction with OH (–R29). The mechanism has a small portion of the NO formed via the pathway NH ⇒ HNO ⇒ NO involving two OH reactions. This pathway for NO formation is probably the most poorly established in the mechanism because the rate constant for NH + OH = HNO + H (R24) may be traced to an estimate (Miller et al. 1983).

The reaction $N_2O + NH = HNO + N_2$ (R41) was also considered in the mechanism. Its rate constant is not well established and the expression used, $k = 2.0 \times 10^{12} e^{-(6{,}000/RT)} cm^3/mol\text{-}s$, was taken from an estimate tabulated in Hanson and Salimian (1985). After consideration, it was excluded from the reaction set since no changes in the major species profiles were observed with its inclusion. There is, however, a slight increase in the NO concentration because of the conversion of HNO to NO and a subsequent decrease in N atoms due to their reaction with NO. Reaction R41 has the largest effect on the HNO concentration which doubles when the reaction is included in the mechanism. The effects of R41 on the HNO and N profiles are shown in Figure 13. The importance of R41 in the mechanism is difficult to assess since the HNO and N radicals could not be measured in the present study and none of the measured species has much sensitivity to the reaction. Therefore, the relative importance of R41 deserves future consideration.

5. CONCLUSION

A combined experimental and detailed chemical modeling study of a stoichiometric $H_2/N_2O/Ar$ flame has been presented. The experiments were performed at low pressure with MB/MS and LIF diagnostic techniques. The low-pressure environment enables the profiles to be examined at higher spatial resolution than has appeared in most of the prior flame studies on this chemical system. In addition, a larger number of species has been measured than in previous studies.

A chemical mechanism for the system was developed by compiling a comprehensive mechanism and then removing unimportant species and most of the unimportant reactions through sensitivity analysis. Pertinent literature was reviewed in order to select the best rate coefficients for the important reactions. In general, the agreement between the model and experiment is acceptable. The chemistry governing the

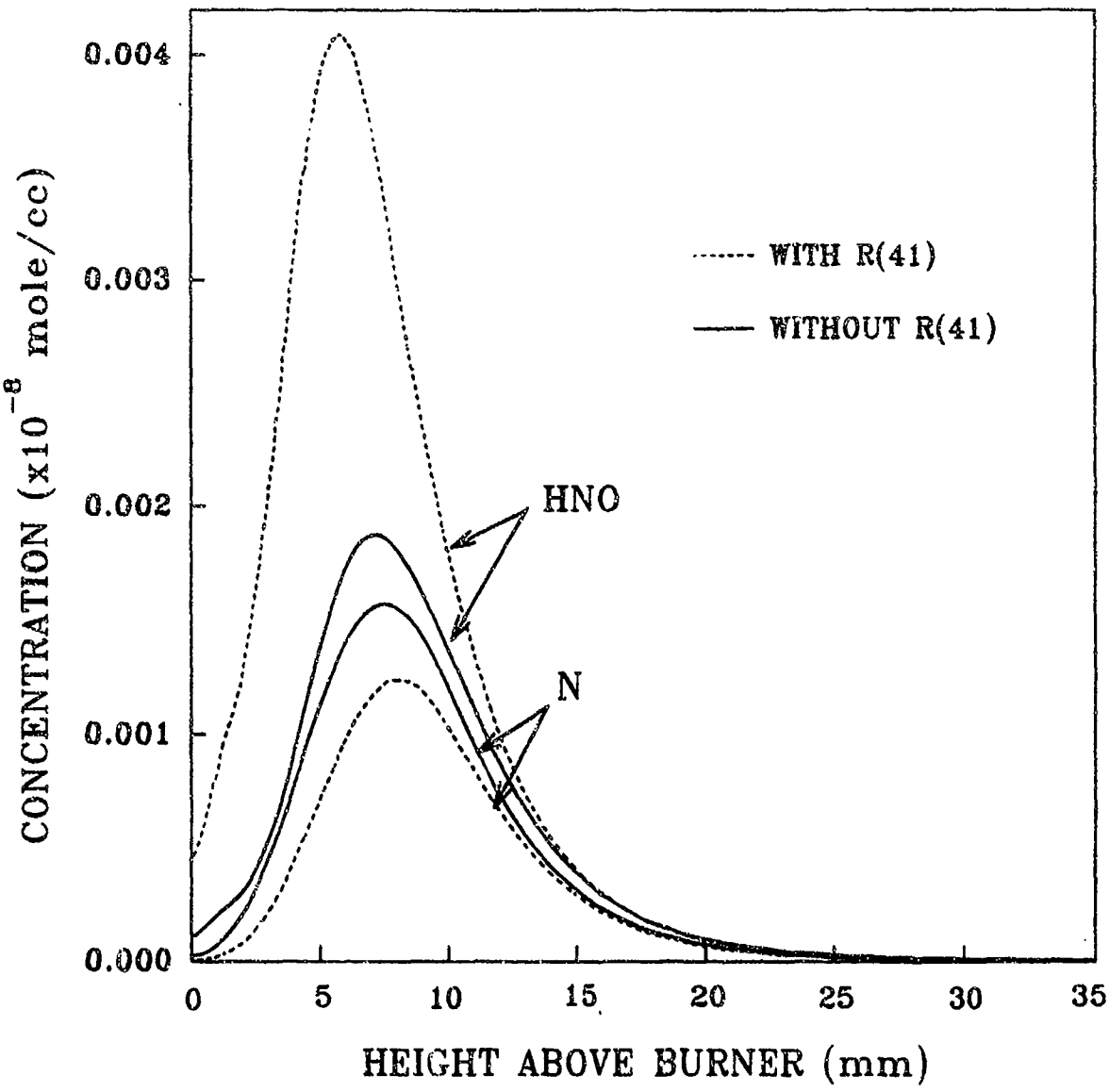

Figure 13. Computed profiles of HNO and N atoms with (dashed line) and without (solid line) reaction $N_2O + NH = HNO + N_2$ (R41).

present flame conditions has been discussed in detail. The main qualitative features of the mechanism have not changed a great deal from previous recommendations. However, several important new findings have been made. First, the possible role of the reaction $N_2O + OH = HO_2 + N_2$ has been investigated. The present results are best modeled if the rate coefficient used is very small; however, a modest rate coefficient may be acceptable. If it is fast enough, this reaction could have important effects on the overall combustion rate under pertinent conditions. Second, the importance of various colliders in the reaction $N_2O + M = N_2 + O + M$ was also considered. Many previous studies have established that this reaction is a major initiation step in the system. Under the present conditions, the most important colliders appear to be N_2O and H_2O. However, this result depends in part on the supposition that the estimated efficiency factor for H_2 is considerably smaller than that of N_2O and H_2O. Third, the present work corroborates the results of other recent studies which indicate that the rate coefficient of the reaction $NH + NO = N_2O + H$ should be larger at high temperature than indicated in previous studies.

INTENTIONALLY LEFT BLANK.

6. REFERENCES

Anderson, W. R. Journal of Physical Chemistry, vol. 93, p. 530, 1989.

Atkinson, R., D. L. Baulch, R. A. Cox, R. F. Hampson Jr., J. A. Kerr, and J. Troe. Journal of Physical and Chemical Reference Data, vol. 18, p. 881, 1989.

Balakhnin, V. P., J. Vandooren, and P. J. Van Tiggelen. Combustion and Flame, vol. 28, p. 165, 1977.

Baldwin, R. R., A. Gethin, J. Plaistowe, and R. W. Walker. Journal Chemical Society Faraday Transactions I, vol. 71, p. 1265, 1975.

Baldwin, R. R., A. Gethin, and R. W. Walker. Journal Chemical Society Faraday Transactions I, vol. 69, p. 352, 1973.

Baulch, D. L., D. D. Drysdale, and D. G. Horne. Evaluated Kinetic Data for High Temperature Reactions, vol. 2, London: Buttersworth, 1973.

Bernstein, J. S., A. Fein, J. B. Choi, T. A. Cool, F. C. Sausa, S. L. Howard, R. J. Locke, and A. W. Miziolek. Combustion and Flame, vol. 92, p. 85, 1993.

Bian, J., J. Vandooren, and P. J. Van Tiggelen. Twenty-First Symposium (International) on Combustion. The Combustion Institute, p. 953, 1986.

Bozzelli, J. W., and A. M. Dean. Private communication, 1993.

Cattolica, R., M. Smooke, and A. Dean. Western States Section Meeting of the Combustion Institute, Paper WSS/CI, p. 82, 1982.

Coffee, T. P. Combustion and Flame, vol. 65, p. 53, 1986.

Coffee, T. P., and J. M. Heimerl. Combustion and Flame, vol. 43, p. 273, 1981.

Coffee, T. P., and J. M. Heimerl. Combustion Science and Technology, vol. 34, p. 31, 1983.

Collin, J., and E. P. Lossing. Journal of Chemical Physics, vol. 28, p. 900, 1958.

Davidson, D. F., and R. K. Hanson. International Journal of Chemical Kinetics, vol. 22, p. 843, 1990.

Dean, A. M. International Journal of Chemical Kinetics, vol. 8, p. 459, 1976.

Dean, A. M., M. Chou, and D. Stern. American Chemical Society Symposium Series, vol. 249, edited by T. M. Sloan, p. 71, 1984.

Dean, A. M., D. C. Steiner, and E. E. Wang. Combustion and Flame, vol. 32, p. 73, 1978.

DeMore, W. B., M. J. Molina, S. P. Sander, D. M. Golden, R. F. Hampson, M. J. Kurylo, C. J. Howard, and A. R. Ravishankara. JPL Publication, p. 8741, Jet Propulsion Laboratory, 1987.

Dixon-Lewis, G., M. M. Sutton, and A. Williams. Combustion and Flame, vol. 8, p. 85, 1964.

Dixon-Lewis, G., M. M. Sutton, and A. Williams. Journal Chemical Society London, p. 5724, 1965.

Dixon-Lewis, G., M. M. Sutton, and A. Williams. Tenth Symposium (International) on Combustion. The Combustion Institute, p. 127, 1965.

Durant, Jr. J. L., and C. M. Rohlfing. Private communication, 1993.

Duval, A., and P. J. Van Tiggelen. Bulletin Academy Royal Belges, vol. 53, p. 366, 1967.

Eckbreth, A. C. Laser Diagnostics for Combustion Temperature and Species. Cambridge, MA: Abacus Press, 1988.

Fifer, R. A. Fundamentals of Solid-Propellant Combustion. Edited by K. Kuo. New York: American Institute of Aeronautics and Astronautics, Inc., 1984.

Fine, B. D., and A. Evans. NASA-TN-D1736, National Aeronautics and Space Administration, Washington, May 1963.

Fristrom, R. M., and A. A. Westenberg. Flame Structure. New York: McGraw-Hill Inc., 1965.

Fueno, T., M. Fukuda, and K. Yokoyama. Chemical Physics, vol. 124, p. 265, 1988.

Gaydon, A. G. The Spectroscopy of Flames. New York: John Wiley & Sons, 1974, and references therein.

Gaydon, A. G., and H. G. Wolfhard. Third Symposium (International) on Combustion. The Combustion Institute, p. 504, 1949.

Gordon, S., W. Mulac, and P. Nangia. Journal of Physical Chemistry, vol. 75, p. 2087, 1971.

Hansen, I., K. Hölinghaus, C. Zetzsch, and F. Stuhl. Chemical Physics Letters, vol. 42, p. 370, 1976.

Hanson, R. K., and S. Salimian. Combustion Chemistry. Edited by W. C. Gardiner. Chapter 6, p. 361. New York: Springer-Verlag New York Inc., 1985.

Harrison, J. A., and R. G. A. R. Maclagan. Journal Chemical Society Faraday Transactions, vol. 86, p. 3519, 1990.

Harrison, J. A., A. R. Whyte, and L. F. Phillips. Chemical Physics Letters, vol. 129, p. 346, 1986.

Henrici, H., and S. H. Bauer. Journal of Chemical Physics, vol. 50, p. 1333, 1969.

Hidaka, Y., H. Takuma, and M. Suga. Journal of Chemical Physics, vol. 89, p. 4903, 1985.

Hidaka, Y., H. Takuma, and M. Suga. Bulletin Chemical Society Japan, vol. 58, p. 2911, 1985.

Howard, S. L., R. J. Locke, R. C. Sausa, and A. W. Miziolek. Rapid Communication Mass Spectrometry, vol. 6, p. 278, 1992.

Jefferies, J. B., K. Kohse-Hoinghaus, G. P. Smith, R. A. Copeland, and D. R. Crosley. Chemical Physics Letters, vol. 152, p. 160, 1988.

Kee, R. J., J. F. Grcar, M. D. Smooke, and J. A. Miller. Sandia Report SAND-85-8240, Sandia National Laboratory, December 1985, reprinted March 1991.

Kee, R. J., G. Dixon-Lewis, J. Warnatz, M. E. Coltrin, and J. A. Miller. Sandia Report SAND-86-8246, Sandia National Laboratory, November 1988.

Kee, R. J., F. M. Rupley, and J. A. Miller. Sandia Report SAND-87-8215, Sandia National Laboratory, December 1987.

Kee, R. J., F. M. Rupley, and J. A. Miller. Sandia Report SAND-89-8009, Sandia National Laboratory, September 1989.

Kent, J. H. Combustion and Flame, vol. 14, pp. 279–281, 1970.

Kohse-Hoinghaus, K., J. Jefferies, R. A. Copeland, G. P. Smith, and D. R. Crosley, Twenty-Second Symposium (International) on Combustion. The Combustion Institute, p. 1857, 1988.

Koshi, M., K. Yoshimura, K. Fukuda, H. Matsui, K. Sait, M. Wantanabe, A. Imamaura, and C. Chen. Journal of Chemical Physics, vol. 93, p. 8703, 1990.

Marshall, P., A. Fontijn, and C. F. Melius. Journal of Chemical Physics, vol. 86, p. 5540, 1987.

Marshall, P., T. Ko, and A. Fontijn. Journal of Physical Chemistry, vol. 93, p. 1922, 1989.

Martin, R. J., and N. J. Brown. Combustion and Flame, vol. 78, p. 365, 1989.

Martin, R. J., and N. J. Brown. Combustion and Flame, vol. 80, p. 238, 1990.

Martin, R. J., and N. J. Brown. Combustion and Flame, vol. 82, p. 312, 1990.

Masten, D. A., R. K. Hanson, and C. T. Bowman. Journal of Physical Chemistry, vol. 94, p. 7119, 1990.

Mertens, J. D., A. Y. Chang, R. K. Hanson, and C. T. Bowman. International Journal of Chemical Kinetics, vol. 21, p. 1049, 1989.

Mertens, J. D., A Y. Chang, R. K. Hanson, and C. T. Bowman. Internal Journal of Chemical Kinetics, vol. 23, p. 173, 1991.

Michael, J. V., and J. W. Sutherland. Journal of Chemical Physics, vol. 92, p. 3853, 1988.

Michaud, M. G., P. R. Westmoreland, and A. S. Feitelburg. To appear in the proceedings, Twenty-Fourth Symposium (International) Combustion. The Combustion Institute, in press.

Miller, J. A. Private communication, 1993.

Miller, J. A., and C. T. Bowman. Progress Energy Combustion Science, vol. 15, p. 287, 1989 and references therein.

Miller, M. S., and A. J. Kotlar. BRL-MR-3545, U. S. Army Ballistic Research Laboratory, Aberdeen Proving Ground, MD, September 1986.

Miller, J. A., and C. F. Melius. Twenty-Fourth Symposium (International) on Combustion. The Combustion Institute, in press.

Miller, J. A., M. D. Smooke, R. M. Green, and R. J. Kee. Combustion Science and Technology, vol. 34, p. 149, 1983.

Pamidimukkala, K. M., and G. B. Skinner. Journal of Chemical Physics, vol. 76, p. 311, 1982.

Peeters, J., and G. Mahnen. Fourteenth Symposium (International) on Combustion. The Combustion Institute, p. 133, 1973.

Peterson, R. C. Ph.D. Thesis, Purdue University, 1981.

Rensberger, K. J., R. A Copeland, M. L. Wise, and D. R. Crosley. Twenty-Second Symposium (International) on Combustion. The Combustion Institute, p. 1867, 1988.

Schoffield, K. comment in J. Bian, J. Vandooren, and P. J. Van Tiggelen. Twenty-First Symposium (International) on Combustion. The Combustion Institute, p. 963, 1986.

Schroeder, M. A. BRL-TR-2659, AD-A159 325, U.S. Army Ballistic Research Laboratory, Aberdeen Proving Ground, MD, June 1985.

Scery, D. J., and M. F. Zabielski. Combustion and Flame, vol. 28, p. 93, 1977.

Smith, G. P. Western States Section Fall Technical Meeting of the Combustion Institute, Berkeley, CA, paper WS92-98, October 1992.

Smith, G. P. Private communication, 1993.

Svehla, R. A., and B. J. McBride. NASA-TN-D-7056, National Aeronautics and Space Administration January 1973.

Thorne, L. R., and C. F. Melius. Proceedings of the Twenty-Sixth JANNAF Combustion Symposium, p. 63, 1989.

Tsang, W., and R. F. Hampson. Journal of Physical and Chemical Reference Data, vol. 15, p. 1087, 1986.

Tsang, W., and J. T. Herron. Journal of Physical and Chemical Reference Data, vol. 20, p. 609, 1991.

Vanderhoff, J. A., S. W. Bunte, A. J. Kotlar, and R. A. Beyer. Combustion and Flame, vol. 65, p. 45, 1986.

Vandooren, J., O. M. Sarkisov, V. P. Balakhnin, and P. J. Van Tiggelen. Chemical Physics Letters, vol. 184, p. 294, 1991.

Walch, S. P. Journal of Chemical Physics, vol. 98, p. 1170, 1993.

Warnatz, J. Berichte der Bunsengellschaft Fuer Physikalische Chemie, vol. 82, p. 834, 1978.

Wolfhard, H. G., and W. G. Parker. Fifth Symposium (International) on Combustion. The Combustion Institute, p. 718, 1955.

Yamasaki, K., S. Okada, M. Koshi, and H. Matsui. Journal of Chemical Physics, vol. 95, p. 5087, 1991.

Yetter, R. A., F. L. Dryer, M Allen, and N. Ilincic. Proceedings of the Twenty-Eighth JANNAF Combustion Symposium, in press.

Yokoyama, K., Y. Sakane, and T. Fueno. Bulletin Chemical Society Japan, vol. 64, p. 1738 1991.

INTENTIONALLY LEFT BLANK.

No. of Copies	Organization
2	Administrator Defense Technical Info Center ATTN: DTIC-DDA Cameron Station Alexandria, VA 22304-6145
1	Commander U.S. Army Materiel Command ATTN: AMCAM 5001 Eisenhower Ave. Alexandria, VA 22333-0001
1	Director U.S. Army Research Laboratory ATTN: AMSRL-OP-CI-AD, Tech Publishing 2800 Powder Mill Rd. Adelphi, MD 20783-1145
1	Director U.S. Army Research Laboratory ATTN: AMSRL-OP-CI-AD, Records Management 2800 Powder Mill Rd. Adelphi, MD 20783-1145
2	Commander U.S. Army Armament Research, Development, and Engineering Center ATTN: SMCAR-IMI-I Picatinny Arsenal, NJ 07806-5000
2	Commander U.S. Army Armament Research, Development, and Engineering Center ATTN: SMCAR-TDC Picatinny Arsenal, NJ 07806-5000
1	Director Benet Weapons Laboratory U.S. Army Armament Research, Development, and Engineering Center ATTN: SMCAR-CCB-TL Watervliet, NY 12189-4050
1	Director U.S. Army Advanced Systems Research and Analysis Office (ATCOM) ATTN: AMSAT-R-NR, M/S 219-1 Ames Research Center Moffett Field, CA 94035-1000

No. of Copies	Organization
1	Commander U.S. Army Missile Command ATTN: AMSMI-RD-CS-R (DOC) Redstone Arsenal, AL 35898-5010
1	Commander U.S. Army Tank-Automotive Command ATTN: AMSTA-JSK (Armor Eng. Br.) Warren, MI 48397-5000
1	Director U.S. Army TRADOC Analysis Command ATTN: ATRC-WSR White Sands Missile Range, NM 88002-5502
(Class only) 1	Commandant U.S. Army Infantry School ATTN: ATSH-CD (Security Mgr.) Fort Benning, GA 31905-5660
(Class only) 1	Commandant U.S. Army Infantry School ATTN: ATSH-WCB-O Fort Benning, GA 31905-5000
1	WL/MNOI Eglin AFB, FL 32542-5000
	Aberdeen Proving Ground
2	Dir, USAMSAA ATTN: AMXSY-D AMXSY-MP, H. Cohen
1	Cdr, USATECOM ATTN: AMSTE-TC
1	Dir, ERDEC ATTN: SCBRD-RT
1	Cdr, CBDA ATTN: AMSCB-CII
1	Dir, USARL ATTN: AMSRL-SL-I
10	Dir, USARL ATTN: AMSRL-OP-CI-B (Tech Lib)

No. of Copies	Organization
1	HQDA, OASA (RDA) ATTN: Dr. C.H. Church Pentagon, Room 3E486 WASH DC 20310-0103
4	Commander US Army Research Office ATTN: R. Chirardelli D. Mann R. Singleton R. Shaw P.O. Box 12211 Research Triangle Park, NC 27709-2211
2	Commander US Army Armament Research, Development, and Engineering Center ATTN: SMCAR-AEE-B, D.S. Downs SMCAR-AEE, J.A. Lannon Picatinny Arsenal, NJ 07806-5000
1	Commander US Army Armament Research, Development, and Engineering Center ATTN: SMCAR-AEE-BR, L. Harris Picatinny Arsenal, NJ 07806-5000
2	Commander US Army Missile Command ATTN: AMSMI-RD-PR-E, A.R. Maykut AMSMI-RD-PR-P, R. Betts Redstone Arsenal, AL 35898-5249
1	Office of Naval Research Department of the Navy ATTN: R.S. Miller, Code 432 800 N. Quincy Street Arlington, VA 22217
1	Commander Naval Air Systems Command ATTN: J. Ramnarace, AIR-5411C Washington, DC 20360
2	Commander Naval Surface Warfare Center ATTN: R. Bernecker, R-13 G.B. Wilmot, R-16 Silver Spring, MD 20903-5000

No. of Copies	Organization
5	Commander Naval Research Laboratory ATTN: M.C. Lin J. McDonald E. Oran J. Shnur R.J. Doyle, Code 6110 Washington, DC 20375
2	Commander Naval Weapons Center ATTN: T. Boggs, Code 388 T. Parr, Code 3895 China Lake, CA 93555-6001
1	Superintendent Naval Postgraduate School Dept. of Aeronautics ATTN: D.W. Netzer Monterey, CA 93940
3	AL/LSCF ATTN: R. Corley R. Geisler J. Levine Edwards AFB, CA 93523-5000
1	AFOSR ATTN: J.M. Tishkoff Bolling Air Force Base Washington, DC 20332
1	OSD/SDIO/IST ATTN: L. Caveny Pentagon Washington, DC 20301-7100
1	Commandant USAFAS ATTN: ATSF-TSM-CN Fort Sill, OK 73503-5600
1	University of Dayton Research Institute ATTN: D. Campbell AL/PAP Edwards AFB, CA 93523
1	NASA Langley Research Center Langley Station ATTN: G.B. Northam/MS 168 Hampton, VA 23365

No. of Copies	Organization
4	National Bureau of Standards ATTN: J. Hastie M. Jacox T. Kashiwagi H. Semerjian US Department of Commerce Washington, DC 20234
1	Applied Combustion Technology, Inc. ATTN: A.M. Varney P.O. Box 607885 Orlando, FL 32860
2	Applied Mechanics Reviews The American Society of Mechanical Engineers ATTN: R.E. White A.B. Wenzel 345 E. 47th Street New York, NY 10017
1	Atlantic Research Corp. ATTN: R.H.W. Waesche 7511 Wellington Road Gainesville, VA 22055
1	Textron Defense Systems ATTN: A. Patrick 2385 Revere Beach Parkway Everett, MA 02149-5900
1	Battelle ATTN: TACTEC Library, J. Huggins 505 King Avenue Columbus, OH 43201-2693
1	Cohen Professional Services ATTN: N.S. Cohen 141 Channing Street Redlands, CA 92373
1	Exxon Research & Eng. Co. ATTN: A. Dean Route 22E Annandale, NJ 08801
1	General Applied Science Laboratories, Inc. 77 Raynor Avenue Ronkonkama, NY 11779-6649

No. of Copies	Organization
1	General Electric Ordnance Systems ATTN: J. Mandzy 100 Plastics Avenue Pittsfield, MA 01203
1	General Motors Rsch Labs Physical Chemistry Department ATTN: T. Sloane Warren, MI 48090-9055
2	Hercules, Inc. Allegheny Ballistics Lab. ATTN: W.B. Walkup E.A. Yount P.O. Box 210 Rocket Center, WV 26726
1	Alliant Techsystems, Inc. Marine Systems Group ATTN: D.E. Broden/MS MN50-2000 600 2nd Street NE Hopkins, MN 55343
1	Alliant Techsystems, Inc. ATTN: R.E. Tompkins 7225 Northland Drive Brooklyn Park, MN 55428
1	IBM Corporation ATTN: A.C. Tam Research Division 5600 Cottle Road San Jose, CA 95193
1	IIT Research Institute ATTN: R.F. Remaly 10 West 35th Street Chicago, IL 60616
2	Director Lawrence Livermore National Laboratory ATTN: C. Westbrook W. Tao, MS L-282 P.O. Box 808 Livermore, CA 94550
1	Lockheed Missiles & Space Co. ATTN: George Lo 3251 Hanover Street Dept. 52-35/B204/2 Palo Alto, CA 94304

No. of Copies	Organization
1	Director Los Alamos National Lab ATTN: B. Nichols, T7, MS-B284 P.O. Box 1663 Los Alamos, NM 87545
1	National Science Foundation ATTN: A.B. Harvey Washington, DC 20550
1	Olin Ordnance ATTN: V. McDonald, Library P.O. Box 222 St. Marks, FL 32355-0222
1	P. J. Gough Associates, Inc. ATTN: P.S. Gough 1048 South Street Portsmouth, NH 03801-5423
2	Princeton Combustion Research Laboratories, Inc. ATTN: N.A. Messina M. Summerfield Princeton Corporate Plaza Bldg. IV, Suite 119 11 Deerpark Drive Monmouth Junction, NJ 08852
1	Hughes Aircraft Company ATTN: T.E. Ward 8433 Fallbrook Avenue Canoga Park, CA 91303
1	Rockwell International Corp. Rocketdyne Division ATTN: J.E. Flanagan/HB02 6633 Canoga Avenue Canoga Park, CA 91304
3	Director Sandia National Laboratories Division 8354 ATTN: S. Johnston P. Mattern D. Stephenson Livermore, CA 94550
1	Science Applications, Inc. ATTN: R.B. Edelman 23146 Cumorah Crest Woodland Hills, CA 91364

No. of Copies	Organization
3	SRI International ATTN: G. Smith D. Crosley D. Golden 333 Ravenswood Avenue Menlo Park, CA 94025
1	Stevens Institute of Tech. Davidson Laboratory ATTN: R. McAlevy, III Hoboken, NJ 07030
1	Sverdrup Technology, Inc. LERC Group ATTN: R.J. Locke, MS SVR-2 2001 Aerospace Parkway Brook Park, OH 44142
1	Sverdrup Technology, Inc. ATTN: J. Deur 2001 Aerospace Parkway Brook Park, OH 44142
3	Thiokol Corporation Elkton Division ATTN: R. Biddle R. Willer Tech Lib P.O. Box 241 Elkton, MD 21921
3	Thiokol Corporation Wasatch Division ATTN: S.J. Bennett P.O. Box 524 Brigham City, UT 84302
1	United Technologies Research Center ATTN: A.C. Eckbreth East Hartford, CT 06108
1	United Technologies Corp. Chemical Systems Division ATTN: R.R. Miller P.O. Box 49028 San Jose, CA 95161-9028
1	Universal Propulsion Company ATTN: H.J. McSpadden 25401 North Central Avenue Phoenix, AZ 85027-7837

No. of Copies	Organization
1	Universal Propulsion Company ATTN: H.J. McSpadden 25401 North Central Avenue Phoenix, AZ 85027-7837
1	Veritay Technology, Inc. ATTN: E.B. Fisher 4845 Millersport Highway P.O. Box 305 East Amherst, NY 14051-0305
1	Brigham Young University Dept. of Chemical Engineering ATTN: M.W. Beckstead Provo, UT 84058
1	California Institute of Tech. Jet Propulsion Laboratory ATTN: L. Strand/MS 125-224 4800 Oak Grove Drive Pasadena, CA 91109
1	California Institute of Technology ATTN: F.E.C. Culick/MC 301-46 204 Karman Lab. Pasadena, CA 91125
1	University of California Los Alamos Scientific Lab. P.O. Box 1663, Mail Stop B216 Los Alamos, NM 87545
1	University of California, Berkeley Chemistry Deparment ATTN: C. Bradley Moore 211 Lewis Hall Berkeley, CA 94720
1	University of California, San Diego ATTN: F.A. Williams AMES, B010 La Jolla, CA 92093
2	University of California, Santa Barbara Quantum Institute ATTN: K. Schofield M. Steinberg Santa Barbara, CA 93106

No. of Copies	Organization
1	University of Colorado at Boulder Engineering Center ATTN: J. Daily Campus Box 427 Boulder, CO 80309-0427
3	University of Southern California Dept. of Chemistry ATTN: R. Beaudet S. Benson C. Wittig Los Angeles, CA 90007
1	Cornell University Department of Chemistry ATTN: T.A. Cool Baker Laboratory Ithaca, NY 14853
1	University of Delaware ATTN: T. Brill Chemistry Department Newark, DE 19711
1	University of Florida Dept. of Chemistry ATTN: J. Winefordner Gainesville, FL 32611
3	Georgia Institute of Technology School of Aerospace Engineering ATTN: E. Price W.C. Strahle B.T. Zinn Atlanta, GA 30332
1	University of Illinois Dept. of Mech. Eng. ATTN: H. Krier 144MEB, 1206 W. Green St. Urbana, IL 61801
1	The Johns Hopkins University Chemical Propulsion Information Agency ATTN: T.W. Christian 10630 Little Patuxent Parkway, Suite 202 Columbia, MD 21044-3200

No. of Copies	Organization
1	University of Michigan Gas Dynamics Lab Aerospace Engineering Bldg. ATTN: G.M. Faeth Ann Arbor, MI 48109-2140
1	University of Minnesota Dept. of Mechanical Engineering ATTN: E. Fletcher Minneapolis, MN 55455
3	Pennsylvania State University Applied Research Laboratory ATTN: K.K. Kuo H. Palmer M. Micci University Park, PA 16802
1	Pennsylvania State University Dept. of Mechanical Engineering ATTN: V. Yang University Park, PA 16802
1	Polytechnic Institute of NY Graduate Center ATTN: S. Lederman Route 110 Farmingdale, NY 11735
2	Princeton University Forrestal Campus Library ATTN: K. Brezinsky I. Glassman P.O. Box 710 Princeton, NJ 08540
1	Purdue University School of Aeronautics and Astronautics ATTN: J.R. Osborn Grissom Hall West Lafayette, IN 47906
1	Purdue University Department of Chemistry ATTN: E. Grant West Lafayette, IN 47906
2	Purdue University School of Mechanical Engineering ATTN: N.M. Laurendeau S.N.B. Murthy TSPC Chaffee Hall West Lafayette, IN 47906
1	Rensselaer Polytechnic Inst. Dept. of Chemical Engineering ATTN: A. Fontijn Troy, NY 12181
1	Stanford University Dept. of Mechanical Engineering ATTN: R. Hanson Stanford, CA 94305
1	University of Texas Dept. of Chemistry ATTN: W. Gardiner Austin, TX 78712
1	Virginia Polytechnic Institute and State University ATTN: J.A. Schetz Blacksburg, VA 24061
1	Freedman Associates ATTN: E. Freedman 2411 Diana Road Baltimore, MD 21209-1525
1	Director Army Research Office ATTN: AMXRO-MCS, K. Clark P.O. Box 12211 Research Triangle Park, NC 27709-2211
1	Director Army Research Office ATTN: AMXRO-RT-IP, Library Services P.O. Box 12211 Research Triangle Park, NC 27709-2211

This Laboratory undertakes a continuing effort to improve the quality of the reports it publishes. Your comments/answers to the items/questions below will aid us in our efforts.

1. ARL Report Number ARL-TR-232 Date of Report October 1993

2. Date Report Received _____

3. Does this report satisfy a need? (Comment on purpose, related project, or other area of interest for which the report will be used.) _____

4. Specifically, how is the report being used? (Information source, design data, procedure, source of ideas, etc.) _____

5. Has the information in this report led to any quantitative savings as far as man-hours or dollars saved, operating costs avoided, or efficiencies achieved, etc? If so, please elaborate. _____

6. General Comments. What do you think should be changed to improve future reports? (Indicate changes to organization, technical content, format, etc.) _____

CURRENT ADDRESS

Organization

Name

Street or P.O. Box No.

City, State, Zip Code

7. If indicating a Change of Address or Address Correction, please provide the Current or Correct address above and the Old or Incorrect address below.

OLD ADDRESS

Organization

Name

Street or P.O. Box No.

City, State, Zip Code

(Remove this sheet, fold as indicated, tape closed, and mail.)
(DO NOT STAPLE)

DEPARTMENT OF THE ARMY

OFFICIAL BUSINESS

BUSINESS REPLY MAIL
FIRST CLASS PERMIT No 0001, APG, MD

Postage will be paid by addressee.

Director
U.S. Army Research Laboratory
ATTN: AMSRL-OP-CI-B (Tech Lib)
Aberdeen Proving Ground, MD 21005-5066

NO POSTAGE
NECESSARY
IF MAILED
IN THE
UNITED STATES